Physica D 240 (2011) 675–693

Contents lists available at ScienceDirect

Physica D

journal homepage: www.elsevier.com/locate/physd

Curvature driven flow of bi-layer interfaces

Nir Gavish, Gurgen Hayrapetyan, Keith Promislow *, Li Yang

Department of Mathematics, Michigan State University, East Lansing, MI 48824, USA

ARTICLE INFO

Article history:
Received 31 May 2010
Accepted 29 November 2010
Available online 10 December 2010
Communicated by J. Bronski

Keywords:
Geometric evolution
Canham–Helfrich energy
Functionalized Cahn–Hilliard energy
Network formation

ABSTRACT

We introduce the Functionalized Cahn–Hilliard (FCH) energy, a negative multiple of the Cahn–Hilliard energy balanced against the square of its own variational derivative, as a finite width regularization of the sharp-interface Canham–Helfrich energy. Mass-preserving gradient flows associated to the FCH energy are higher-order phase field models which develop not only single-layer, or front-type interfaces, but also bi-layer, or homoclinic interfaces with associated endcap and multi-junction structures. The single-layer interfaces manifest a fingering instability which grows into endcapped bi-layers. The meandering growth of the bi-layer interfaces and the subsequent merging lead to a multi-junction dominated network that bears a striking similarity to the phase separated domains of both perfluorosulfonic membranes and amphiphilic di-block co-polymer solutions. The bi-layers generated by the gradient flows of the FCH energy have an interfacial width which scales with $\varepsilon \ll 1$, however for fixed ε, there is a class of bi-layers parameterized by width and background state. Our primary result is the asymptotic derivation of the normal velocity of a closed bi-layer hypersurface in $\mathbb{R}^d$ $(d \geq 2)$ coupled to the evolution for the surface width, curvature, and background state. We also show the convergence of the FCH energy to a scaled Canham–Helfrich type energy for both single and bi-layer interfaces, with the surface area coefficient of the limiting Canham–Helfrich energy coupling to the bi-layer width. Thus the bi-layer networks grow to maximize surface area while minimizing the square of curvature, up to the point that the increase in surface area stretches the bi-layers too thin.

© 2010 Elsevier B.V. All rights reserved.

1. The functionalized Cahn–Hilliard energy

The controlled generation of self-organized, nanoscale networks from coarser mixtures is central to polymer chemistry. One mechanism to generate such networks is through the "functionalization" of hydrophobic polymer chains and nanoparticles by the addition of acid or alkaline tipped side-chains. In the presence of a polar solvent the end groups interact exothermically, driving the spontaneous generation of polymer–solvent or nanoparticle–solvent interfaces. The resulting phase separated network structures can be exploited for charge selective conduction, and have important applications to efficient energy conversion devices such as polymer electrolyte membranes for fuel cells, [1,2], dye sensitized solar cells [3], and bulk-heterojunction solar cells, [4,5].

The phase separation of microemulsions is typically dominated by interfacial energies. The Canham–Helfrich free energy, [6,7], is a sharp interface model which characterize interfaces by their intrinsic properties of surface area and curvature. In three space dimensions the Canham–Helfrich energy of an interface Γ is written in terms of its mean, H, and Gaussian, K, curvatures and its surface area,

$$\mathcal{E}_{CH}(\Gamma) = \int_\Gamma a_1 + a_2(H - a_3)^2 + a_4 K \, \mathrm{d}S. \tag{1.1}$$

The parameter, a_1, denotes the energy density per unit surface area while a_2 and a_4, denote the energy density attributed to the curvatures, with a_3 specifying the intrinsic, or zero-energy, value of the mean curvature. The contribution from the Gaussian curvature over a closed interface depends only upon the interface's Euler characteristic, and neglecting changes in topological type, its surface integral is independent of Γ. An extension of the Canham–Helfrich energy has been proposed by Gurtin and Jabbour, [8], who include regularizations for sharp corners which may arise at grain boundary intersections in crystalline materials. However for soft-condensed matter, the Canham–Helfrich energy is broadly considered to be generic, [9]. An important limitation of a sharp-interface model, particularly when considering the casting of polymer–solvent mixtures, is the need both to couple the interfacial energy to physics outside the interface, such as energy and momentum balance equations, and more importantly, to track interfaces through merging and pinch-off events. Moreover, the Canham–Helfich energy cannot predict the dependence of its parameters upon the interfacial structure, these exigencies are beyond the scope of sharp-interface models.

* Corresponding author. Tel.: +1 517 432 7135; fax: +1 517 432 1562.
E-mail address: kpromisl@math.msu.edu (K. Promislow).

0167-2789/$ – see front matter © 2010 Elsevier B.V. All rights reserved.
doi:10.1016/j.physd.2010.11.016

Phase-field models can be viewed as regularizations of sharp-interface energies that afford a finite interfacial width while naturally accommodating both topological change in interfacial structure and coupling to the physics of the environment in which they are immersed, [10,11]. Chief among these models is the Cahn–Hilliard equation, [12], which describes the phase separation and domain coarsening of binary mixtures of inert materials. It is a mass-conserving H^{-1} gradient flow on a free energy functional of Cahn–Hilliard type

$$\mathcal{E}(u) = \int_\Omega \frac{\varepsilon^2}{2}|\nabla u|^2 + W(u)\,\mathrm{d}x. \tag{1.2}$$

Here u is a scalar quantity representing mixture volume fraction over a domain $\Omega \subset \mathbb{R}^d$, $d \geq 2$. For an appropriate choice of double well potential W, solutions of the Cahn–Hilliard equation rapidly undergo a spinodal decomposition into "pure states" or "phases" occupying respective minima of wells of W, separated by transition layers of $O(\varepsilon)$ thickness. The question of the evolution of the spatial domains occupied by the respective phases has received considerable attention, with Pego first establishing the motion of the interfaces through a Mullins–Sekerka type flow, [13]. He introduced the chemical potential as the solution of Laplace's equation on each spinodal domain with the interfacial curvature as a Dirichlet condition on the internal interfaces. For $\varepsilon \ll 1$ he showed that the leading order normal velocity of the interface of the spinodal domains can be obtained from the jump in the normal derivative of the chemical potential defined on the complementary domains. More rigorous derivations of Pego's results quickly followed, particularly [14] and later [15]. Around the same time, the Γ convergence of the Cahn–Hilliard energy to the surface area functional, that is the Canham–Helfrich energy with $a_2 = a_4 = 0$, was rigorously established, [16,17].

While mixtures of inert materials generically seek to minimize surface area, functionalized materials have embedded charged groups which interact exothermically with polar solvents, spontaneously generating polymer–solvent interface. A prime example is Nafion, a functionalized fluorocarbon polymer frequently used as a membrane separator in polymer electrolyte membrane fuel cells. From their small angle X-ray scattering (SAXS) experiments, [18], Hsu and Gierke hypothesized that the water domain within the Nafion forms small 4–5 nanometer balls interconnected by thin 1–2 nanometer cylindrical pores. They further suggested such a network could arise from a balance between the elastic energy of the interface and the hydrophilic surface interactions among the charged functional groups and the solvent, [18]. There has since been considerable numerical and experimental investigation of the microstructure of Nafion and other perfluorinated membanes, [1,19–24], with a variety of possible morphologies postulated to explain the available data.

We propose a model for interfacial development in functionalized polymer-solvent mixtures which is a regularization of the Canham–Helfrich energy. The model affords a finite interfacial width, accommodates merging and other topological reorganization, and couples naturally to momentum balance and other macroscopic mass transport equations. We assign a negative value to interfacial energy via the Cahn–Hilliard energy, and balance the negative Cahn–Hilliard energy against the square of its own variational derivative. In general, we denote such an energy, $\mathcal{F}$, the *functionalization* of the original energy, $\mathcal{E}$,

$$\mathcal{F}(u) = \int_\Omega \frac{1}{2}\left(\frac{\delta \mathcal{E}}{\delta u}(u)\right)^2 \mathrm{d}x - \eta\,\mathcal{E}(u). \tag{1.3}$$

In particular the Functionalized Cahn–Hilliard (FCH) energy takes the form

$$\mathcal{F}(u) = \int_\Omega \frac{1}{2}\left(\varepsilon^2\Delta u - W'(u)\right)^2 - \eta\left(\frac{\varepsilon^2}{2}|\nabla u|^2 + W(u)\right)\mathrm{d}x, \tag{1.4}$$

where W is a smooth, double-well potential with *equal* global minima at states $u = b_\pm$, with $b_- < b_+$ and $\mu_\pm \equiv W''(b_\pm) > 0$. Without loss of generality, we assume $W(b\pm) = 0$. Viewing the square of the first variation as the bending energy of the interface, physical considerations suggest the constant $\eta > 0$ be small since bending energy typically dominates the hydrophilic surface energy; for mathematical reasons it is natural to scale η as $\eta = \varepsilon^2\eta_2$ where η_2 is positive and independent of ε. It has been demonstrated for a broad class of energies that their associated functionalized form is bounded below and possesses global minimizers over natural function spaces, [25]. An energy similar to the FCH, called the Φ^6 model, has been proposed for amphiphilic systems, in which two immiscible fluids are mixed with a surfactant forming a microemulsion at the interface, [26]. The Φ^6 model was motivated by SAXS data which can be related to the reciprocal of the Fourier transform of the second variation of the energy evaluated at a constant background state. The De Giorgi conjecture, concerning the Γ-convergence of (1.4) in the case $\eta = -\varepsilon^2$, when both terms are positive, has recently been established, [27]; however the nature of the energy and the dynamics of the associated gradient flows are substantially different in the case $\eta > 0$.

This paper concerns the long-time evolution of the zero-mass projection gradient flow of the FCH energy on a periodic domain $\Omega \subset \mathbb{R}^d$ for $d \geq 2$,

$$u_t = -\Pi_0 F(u), \tag{1.5}$$

$$u(x, 0) = u_0(x), \tag{1.6}$$

where F is the first variation of the FCH energy. It is significant that F factors into a constant offset of the second variation of $\mathcal{E}$ acting on the first variation of $\mathcal{E}$,

$$\begin{aligned} F(u) \equiv \frac{\delta \mathcal{F}}{\delta u} &= \left(\frac{\delta^2 \mathcal{E}}{\delta u^2} + \varepsilon^2\eta_2\right)\frac{\delta \mathcal{E}}{\delta u} \\ &= \left(\epsilon^2\Delta - W''(u) + \varepsilon^2\eta_2\right)\left(\epsilon^2\Delta u - W'(u)\right). \end{aligned} \tag{1.7}$$

We also introduce the zero-mass projection

$$\Pi_0 f \equiv f - \langle f\rangle_\Omega\,, \tag{1.8}$$

which is the complement of the average value operator

$$\langle f\rangle_\Omega \equiv \frac{1}{|\Omega|}\int_\Omega f(x)\,\mathrm{d}x. \tag{1.9}$$

The evolution of the zero-mass projection functionalized Cahn–Hilliard (ZMFCH) equation preserves the mass of the initial data, $\frac{\mathrm{d}}{\mathrm{d}t}\langle u\rangle_\Omega = 0$, while decreasing the FCH energy, $\frac{\mathrm{d}}{\mathrm{d}t}\mathcal{F}(u) \leq 0$. Analysis of the zero-mass projection gradient flow of the Cahn–Hilliard energy may be found in [28].

Fig. 1.1 depicts the spontaneous network formation in $\Omega \subset \mathbb{R}^2$ which is typical of the ZMFCH equation. Reading left to right, the initial data is four circles of "water" ($u = b_+$) within a background of "polymer" ($u = b_-$). The boundary between the two domains is given by a front-type or single-layer interface which the FCH shares with the Cahn–Hilliard energy. The higher curvature circles grow at the expense of the lower curvature ones, however, as can be seen in the second frame, the circular domains are unstable to an antipodal elongation. The elongated circle assumes a dumbbell shape which stretches and merges with the adjacent circles in frames 3 and 4, forming a narrow bi-layer, capped by two semi-circular endcaps. Cross sections of the bi-layer show a homoclinic or bi-layer structure. Progressing from frame 5 to 6 and 7, the bi-layer begins to narrow as it stretches and meanders, meanwhile

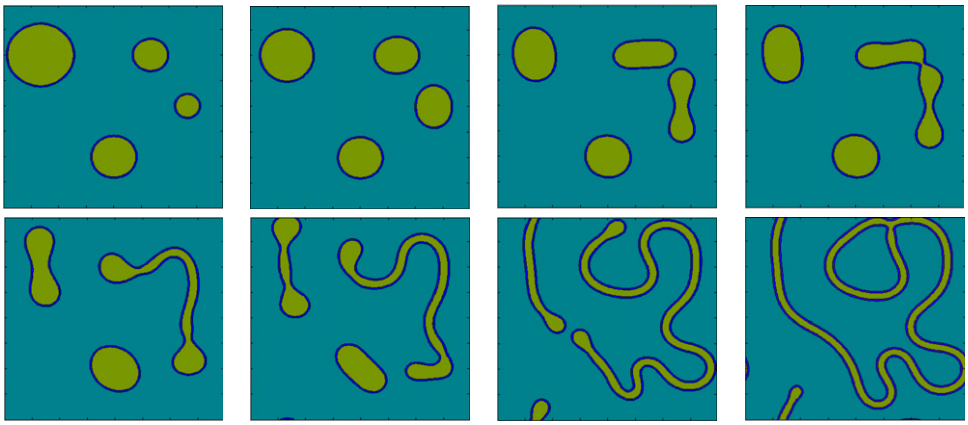

Fig. 1.1. Spontaneous network generation in the gradient flow (1.5) from an initial data consisting of four circular masses. Time evolution (left to right) for a simulation with $\varepsilon = 0.03$ and $\eta = \varepsilon^2$. The blue and red domains correspond to the regions where $u(x)$ resides at one of the two minima of the potential well $W(s) = (1 - s^2)^2/4$.

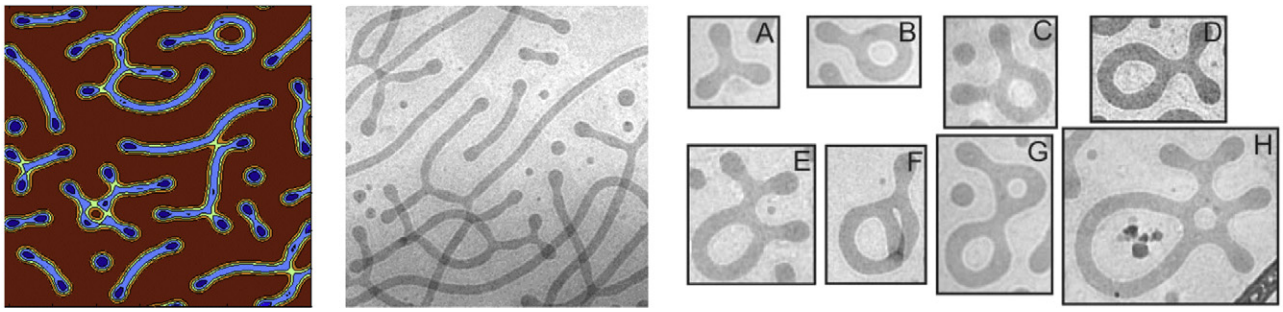

Fig. 1.2. (Left) Quasi-steady equilibrium of the ZMFCH with the classic double well $W = (1 - s^2)^2/4$, $\varepsilon = 0.03$, and $\eta = 4\varepsilon^2$. The solution was obtained from long time ($t = O(\varepsilon^{-4})$) evolution from random initial data, $u_0 = \pm 1$ with $\Pi_0 u_0 = 0.6|\Omega|$, or roughly 20% $u = -1$. (Center and Right) Amphiphilic di-block co-polymer mixtures of Polyethylene oxide and Polybutadiene, from [31,32] respectively, with a higher concentration of functional groups in the right-most figure.

the endcaps intersect and merge with the other domains. Finally, in frame 8, we find a single meandering bi-layer with a triple junction and one endcap. The bi-layer is sufficiently thin that the resulting structure is stationary, at least up to times t of $O(\varepsilon^{-4})$, as compared to the $t = O(\varepsilon^{-3})$ evolution depicted in frames 1–8.

1.1. Summary of results

We consider a closed hypersurface Γ with curvatures and surface area uniformly bounded with respect to $\varepsilon \ll 1$, and which is far from self-intersection when distance is measured in units of ε. We "dress" such hypersurfaces with either a single or a bi-layer interfacial structure. We do not consider hypersurfaces with boundary or self-intersection, which excludes endcaps and multi-junctions. The construction of the bi-layer interfaces is the re-formulation of the fourth-order FCH energy as a square of a second order energy plus an $O(\varepsilon^2)$ zeroth order perturbation, (4.9). At the leading order in the transverse variable, the second order energy supports heteroclinic connections which are degenerate, and can be unfolded at $O(\varepsilon)$ into a family of homoclinic bi-layer solutions parameterized by a detuning parameter α that is inversely related to the bi-layer width, (4.13), and a background state b. While α and b are independent in the leading order construction, we show in Proposition 4.1 that if α and b are properly related then the leading order term can be extended to a 1D homoclinic solution. The unfolding is generic for functionalized energies, arising from the factored form of the first variation of a functionalized energy. The unfolding of a heteroclinic orbit into a homoclinic orbit (a front and a back) has been studied in detail [29,30] in the well-separated limit, corresponding to $|\ln \varepsilon| \gg 1$, for which the homoclinics are exponentially close to equilibrium at the plateau. For the bi-layer interfaces, we construct homoclinics which are $O(\sqrt{\varepsilon})$ away from the equilibrium value at the pulse maximum, and show that the ground state eigenvalue of the corresponding linear operator is $O(\varepsilon)$. Within this regime we demonstrate that as $\varepsilon \to 0^+$ the FCH energy evaluated at a dressed hypersurface converges to a Canham–Helfrich energy, see (3.3) and (4.65). In particular for the bi-layer interfaces, the limiting surface area term, a_1 depends upon the value of the detuning parameter, becoming positive if the bi-layer is sufficiently narrow (see Fig. 1.2).

Our main result concerns solutions of the ZMFCH Eq. (1.5) which start sufficiently close to either a single-layer or bi-layer dressing of a hypersurface Γ. We show that as long as the curvatures of Γ remain bounded and Γ remains far from self-intersection, then the flow under (1.5) can be reduced to an evolution of the hypersurface, through its normal velocity, coupled to evolution equations for the interfacial parameters, which may vary in time and with position along the interface. For a single-layer interface, we uncover a two time-scale evolution. On the fastest time scale, $t = O(\varepsilon^{-1})$, the spatially constant background state is driven to a value determined by a weighted integral of the normal velocity over the hypersurface. The normal velocity is manifest on the slower time-scale, $t = O(\varepsilon^{-3})$, on which the adiabatically driven background adjusts to maintain a zero average value for the normal velocity over the interface. In $\mathbb{R}^3$, the leading order normal velocity is given by

$$\mathbf{V}_n = 2\Pi_{0,\Gamma}\left(\Delta_s + \eta_2 + 2H^2 - 2K\right)H + O(\varepsilon), \tag{1.10}$$

where $\Pi_{0,\Gamma}$ is the zero-mass projection operator over the hypersurface Γ, the parameter $\eta = \varepsilon^2\eta_2$, $H = \frac{1}{2}(k_1 + k_2)$ and $K = k_1k_2$ are the mean and Gaussian curvatures, and Δ_s is the Laplace–Beltrami or surface diffusion operator on Γ. In particular in two dimensions we show that circular interfaces are linearly unstable

to anti-podal stretching modes if the curvature is too small, as measured against η_2, see (3.42).

The evolution of a bi-layer dressed hypersurface couples more subtly to the parameters, with three relevant time-scales. At the fastest time-scale, $t = O(\varepsilon^{-1})$, the spatially constant background state is determined by a weighted average value of the bi-layer width over the hypersurface Γ. At the second fastest time-scale, $t = O(\varepsilon^{-2})$, the adiabatically driven background state adjusts so that the detuning parameter, α, satisfies a nonlocal–nonlinear differential equation (5.35). We show this system has a linearly stable family of spatially constant solutions (independent of position along Γ), and that the value of the constant depends only upon the area of the hypersurface Γ and the conserved total mass of the initial data. The normal velocity is manifest at the slowest time-scale, $t = O(\varepsilon^{-3})$, which is also the time-scale depicted in Fig. 1.1. The normal velocity is determined by the curvatures of the hypersurface and the value of the detuning parameter, which in turn evolves as the interfacial area changes under its normal velocity. In $\mathbb{R}^3$ the normal velocity takes the form

$$\mathbf{V}_n = 2\left(\Delta_s - \beta(\alpha) + 2H^2 - 2K\right)H + O(\varepsilon), \tag{1.11}$$

where the coupling parameter β, given in (5.65) and more explicitly in (5.66), approaches $-\eta_2$ for wide bi-layers ($\alpha \ll 1$) and generically becomes positive as the bi-layer width decreases (α increases). The increase in β is associated with an arresting of the growth of the interfacial area. In particular, taking Γ to be radially symmetric in $\mathbb{R}^3$, and fixing the total mass, then the equilibrium value of α satisfies $\beta(\alpha) = 0$, with the radius R determined by the mass constraint. For $d \neq 3$ the full system is given by (5.79). Moreover we demonstrate that these equilibrium configurations are linearly stable to non-radial perturbations of the interfacial shape Γ. In two space dimensions we more fully characterize stationary interfaces in terms of a second order differential equation in arc-length. In particular, for $\beta > 0$, this curvature equation has a symmetric figure-eight orbit homoclinic to the origin which is surrounded by hour-glass shaped periodic orbits. The periodic orbits give the curvature as a function of arc-length, and the integration of these curvatures yields two-dimensional curves. For periodic orbits that are sufficiently far outside the homoclinic, the resulting curves are non-self intersecting. Moreover these curves evidence a meander pattern which is a generic feature of the ZMFCH flows, for example it is readily identifiable in the bottom-right section of the interfacial structure in frame 8 of Fig. 1.1, and is shown in detail in Fig. 5.3.

2. Whiskered coordinates in $\mathbb{R}^d$

We define admissible interfaces to be smooth, closed (compact and without boundary), orientable hypersurfaces $\gamma : S \subset \mathbb{R}^{d-1} \to \mathbb{R}^d$ which are far from self-intersection when distance is measured in units of ε. For such an interface we introduce the whiskered coordinates in a neighborhood of $\Gamma = \gamma(S)$. Although these coordinates have been introduced before in the context of geometric evolution, see [33] for example, their application to the fourth-order problems hinges upon higher order terms which we make precise in this section. We introduce the diffeomorphic change of variables $\varphi : (s, z) \to x$, defined by

$$\varphi(s, z) = \gamma(s) + \epsilon z \nu(s), \tag{2.1}$$

where the *Gauss map*, $\nu : S \to S^{d-1}$, gives the outward pointing unit normal vector perpendicular to the tangent hyperplane to Γ at $\gamma(s)$. This change of variables is valid in the neighborhood

$$\Gamma(L) \equiv \{\varphi(s, z) | s \in S, -L/\epsilon \leq z \leq L/\epsilon\}, \tag{2.2}$$

of Γ, so long as L is sufficiently small, as measured against the H^1 norm of γ, but independent of ε. We will call the line segments $\{\gamma(s) \times [-L/\varepsilon, L/\varepsilon] | s \in \Gamma\}$ the *whiskers* of γ, and refer to (s, z) as the whiskered coordinate system.

The Laplacian takes a particularly instructive form in the whiskered coordinates. Introducing the variables $y = (s_1, \ldots, s_{d-1}, z)$ then $x = \varphi(y)$ and the y coordinates are a chart for $\Gamma(L)$, and the Laplace–Beltrami formulation for the Laplacian is given by

$$\Delta \equiv \frac{1}{\sqrt{\det(\mathbf{g})}} \sum_{i=1}^{d} \sum_{j=1}^{d} \frac{\partial}{\partial y_i} (\mathbf{g}^{-1})_{ij} \sqrt{\det(\mathbf{g})} \frac{\partial}{\partial y_j}, \tag{2.3}$$

where $\mathbf{g}$ is the metric tensor,

$$g_{ij} = \left\langle \frac{\partial x}{\partial y_i}, \frac{\partial x}{\partial y_j} \right\rangle_{\mathbb{R}^d}. \tag{2.4}$$

Letting $\mathbf{J}$ denote the Jacobian matrix for (2.1), we have,

$$\mathbf{g} = \mathbf{J}^{\mathbf{T}}\mathbf{J}, \tag{2.5}$$

and consequently, $\det(\mathbf{g}) = J^2$, where $J = J(s, z)$ is the associated Jacobian. We may also write,

$$\mathbf{g} = \begin{pmatrix} \mathbf{g_0} & 0 \\ 0 & \epsilon^2 \end{pmatrix} \tag{2.6}$$

where $\mathbf{g_0}(s, 0)$ is the metric tensor for the hyperplane Γ. In the whiskered variables the Laplacian takes the form,

$$\Delta = \epsilon^{-2} J^{-1} \frac{\partial}{\partial z} J \frac{\partial}{\partial z} + \Delta_s, \tag{2.7}$$

where Δ_s is the Laplace–Beltrami operator when restricted to act on Γ,

$$\Delta_s = \frac{1}{\sqrt{\det(\mathbf{g}_0)}} \sum_{i=1}^{d-1} \sum_{j=1}^{d-1} \frac{\partial}{\partial s_i} \left(\mathbf{g}_\mathbf{0}^{-1}\right)_{ij} \sqrt{\det(\mathbf{g}_0)} \frac{\partial}{\partial_{s_j}}. \tag{2.8}$$

We also introduce the tangential gradient,

$$|\nabla_s f|^2 = \sum_{i,j=1}^{d-1} (\mathbf{g}_0)_{ij} \frac{\partial f}{\partial s_i} \frac{\partial f}{\partial s_j}. \tag{2.9}$$

To simplify the z derivatives in (2.7) we derive an expression for J in terms of the principal curvatures $\{k_i\}_{i=1}^{d-1}$ of Γ. We first observe that,

$$\frac{\partial \varphi}{\partial s_i} = \frac{\partial \gamma}{\partial s_i} + \epsilon z \frac{\partial \nu}{\partial s_i} = \frac{\partial \gamma}{\partial s_i} + \epsilon z \sum_{j=1}^{d-1} \frac{\partial \gamma}{\partial s_j} b_{ji}, \tag{2.10}$$

where $\mathbf{B} \equiv (b)_{ij}$ is the Weingarten matrix whose elements satisfy,

$$\frac{\partial \nu}{\partial s_i} = \sum_{j=1}^{d-1} \frac{\partial \gamma}{\partial s_j} b_{ji}. \tag{2.11}$$

The eigenvalues of B are necessarily real, and are by definition the principal curvatures of Γ. From (2.10) we see that the Jacobian matrix takes the form,

$$\mathbf{J} = \overbrace{\begin{pmatrix} \frac{\partial \gamma}{\partial s_1} & \frac{\partial \gamma}{\partial s_2} & \cdots & \frac{\partial \gamma}{\partial s_{d-1}} & \nu \end{pmatrix}}^{\mathbf{J}(s,0)} \begin{pmatrix} I_{d-1} + \varepsilon z B & 0 \\ 0 & \epsilon \end{pmatrix}, \tag{2.12}$$

where I_{d-1} is the $d-1 \times d-1$ identity matrix. Without loss of generality, for a sufficiently smooth curve Γ we may choose a parameterization γ for which $\det \mathbf{J}(s, 0) = 1$. Taking the determinant of the Jacobian matrix yields

$$J(s, z) = \det \mathbf{J} = \varepsilon \det(I + \epsilon z \mathbf{B}) = \varepsilon \prod_{i=1}^{d-1} (1 + \epsilon z k_i)$$

$$= \sum_{j=0}^{d} \varepsilon^{j+1} K_j z^j, \tag{2.13}$$

where $K_0 = 1$ and $K_i \equiv \sum_{j_1<\cdots<j_i} k_{j_1}\cdots k_{j_i}$ is the ith Gaussian curvature of Γ. Taking the z derivative of the product form of the Jacobian expression in (2.13) we obtain the identity,

$$J_z = \epsilon^2 \sum_{i=1}^{d-1} k_i \prod_{j\neq i}(1+\epsilon z k_j) = \varepsilon\kappa J, \tag{2.14}$$

where the extended curvature

$$\kappa(s,z) \equiv J_z/(\epsilon J) = \sum_{i=1}^{d-1} \frac{k_i}{1+\epsilon z k_i} = \sum_{j=0}^{\infty} \kappa_j \epsilon^j z^j, \tag{2.15}$$

is expressed in terms of the coefficients

$$\kappa_j(s) = (-1)^j \sum_{i=1}^{d-1} k_i^{j+1}(s). \tag{2.16}$$

We call this the extended mean curvature since $\kappa = \nabla_x \cdot \nu$ is the Cartesian divergence of the normal to Γ when the normal is extended off of Γ as a constant along whiskers. We remark that while the Jacobian remains smooth, in fact it is a polynomial in z, the extended curvature becomes singular when the whiskers intersect. Distributing the z derivative in (2.7) and using the identity (2.14) yields the desired change of variables

$$\Delta_x = \epsilon^{-2}\partial_z^2 + \epsilon^{-1}\kappa(s,z)\partial_z + \Delta_s. \tag{2.17}$$

2.1. Dressed interfaces and other notation

A function $f(x)$ which decays exponentially to zero away from a front Γ at an $O(1)$ rate in z will be said to be "localized on the surface" or merely "localized". Up to exponentially small terms localized functions can be written in the whiskered variables, so that $f(x) = f(s,z)$. Functions $h(z)$ of one variable which decay exponentially to constant values at $\pm\infty$ can be extended to Ω by setting them to their limiting value for $|z| > 2L/\varepsilon$ and smooth for $|z| \in (L/\varepsilon, 2L/\varepsilon)$. The expression *the hypersurface Γ dressed by h* refers to the extended function $h(x)$, understood to mean $h(z(x))$.

The L^2 norm over Ω or Γ will be denoted by $\|f\|_{L^2(\Omega)}$ or $\|f\|_{L^2(\Gamma)}$ respectively. The L^2 inner product of a localized function over a particular whisker will be unadorned,

$$(f,g)_2(s) = \int_{\mathbb{R}} f(s,z)g(s,z)\,\mathrm{d}z, \tag{2.18}$$

where it is understood that we extend localized functions by zero off of $\Gamma(2L)$. The corresponding whiskered L^2 norm is denoted $\|f\|_2$. Volume integrals of f in the whiskered variables take the form

$$\int_{\Gamma(L)} f(x)\,\mathrm{d}x = \int_\Gamma \int_{-L}^{L} f(s,z)J(s,z)\,\mathrm{d}z\,\mathrm{d}s. \tag{2.19}$$

When f is localized about Γ the whisker integral can be approximated by the integral over all $\mathbb{R}$ as

$$\int_{\Gamma(L)} f(x)\,\mathrm{d}x = \int_\Gamma \int_{\mathbb{R}} f(s,z)J(s,z)\,\mathrm{d}s\,\mathrm{d}z, \tag{2.20}$$

up to exponentially small terms. Moreover we define the *whiskered mass* $\bar f$ of a localized function f as

$$\bar f(s) \equiv \int_{\mathbb{R}} f(z,s)\,\mathrm{d}z. \tag{2.21}$$

Derivatives of a function of one variable, or of a function with a "dominant" variable will be denoted with a prime. For example, given $\phi = \phi(z;\alpha)$ a function of z parameterized by α, the partial of ϕ with respect to z will be denoted by ϕ'. For a function f which decays exponentially to unequal limits in z, we denote the jump of f across a given whisker by

$$[\![f]\!](s) = f(s,\infty) - f(s,-\infty). \tag{2.22}$$

A function f which decays exponentially to a constant background b as $z \to \pm\infty$ can be broken into a "near-field" piece, $f - b$, which is localized, and a "far-field" constant b. We will use γ and ρ with subscripts to denote constants which are positive, $O(1)$, and independent of ε and other parameters (especially the detuning α and background b) to leading order.

3. Geometric evolution of single layer interfaces

Fix an admissible interface Γ. We wish to consider a potential minimizer of (1.4) obtained by dressing Γ with a 1D front solution, which we search for among the unconstrained critical points of $\mathcal{F}$. Such critical points solve $F(u) = 0$, where F is given by (1.7), and a natural choice for an approximate critical point is the critical point $\phi_{\mathrm{f}}(z)$ of the Cahn–Hilliard energy given by

$$\partial_z^2\phi_{\mathrm{f}} - W'(\phi_{\mathrm{f}}) = 0, \tag{3.1}$$

subject to $\phi_{\mathrm{f}} \to b_\pm$ as $z \to \pm\infty$. From the change of variables (2.1) we may smoothly extend ϕ_{f} to all of Ω. To derive a connection between the FCH energy (1.4) and the Canham–Helfrich energy (1.1) we use the whiskered coordinates to expand $\mathcal{F}$,

$$\mathcal{F}(\phi_{\mathrm{f}}) = \int_\Gamma \int_{\mathbb{R}} \Bigg[\frac{1}{2}\left(\partial_z^2\phi_{\mathrm{f}} + \varepsilon\kappa\partial_z\phi_{\mathrm{f}} + \varepsilon^2\Delta_s\phi_{\mathrm{f}} - W'(\phi_{\mathrm{f}})\right)^2 - \eta\left(\frac{1}{2}|\partial_z\phi_{\mathrm{f}}|^2 + \varepsilon^2|\nabla_s\phi_{\mathrm{f}}|^2 + W(\phi_{\mathrm{f}})\right)\Bigg] J(s,z)\,\mathrm{d}s\,\mathrm{d}z. \tag{3.2}$$

However ϕ_{f} is independent of the tangential variables s, so the tangential gradient and Laplace–Beltrami terms are zero. Scaling $\eta = \varepsilon^2\eta_2$ and integrating (3.1) to obtain the point-wise equality $\frac{1}{2}|\phi_{\mathrm{f}}'|^2 = W(\phi_{\mathrm{f}})$, we find

$$\begin{aligned}\lim_{\varepsilon\to 0^+} \varepsilon^{-3}\mathcal{F}(\phi_{\mathrm{f}}) &= \|\phi_{\mathrm{f}}'\|_2^2 \int_\Gamma \frac{1}{2}\kappa_0^2 - \eta_2\,\mathrm{d}s, \\ &= \|\phi_{\mathrm{f}}'\|_2^2 \int_\Gamma \left[\frac{(d-1)^2}{2}H^2 - \eta_2\right]\mathrm{d}s,\end{aligned} \tag{3.3}$$

which is a Canham–Hilfrich energy with zero intrinsic and Gaussian curvatures.

3.1. Fully dressed, single-layer Ansatz

To resolve the geometric evolution an admissible interface Γ under the zero-mass gradient descent (1.5) we construct the following fully-dressed, single-layer Ansatz

$$\Phi_{\mathrm{f}}(s,z) = \phi_{\mathrm{f}}(z) + \epsilon^2\phi_2(s,z) + \varepsilon^3 b_3, \tag{3.4}$$

where the second order term ϕ_2 is chosen to reduce the size of the residual and incorporates curvature dependent corrections. The scalar parameter $b(t) = b_- + \varepsilon^3 b_3(t)$ is a perturbation to the spatially constant background state. We also introduce the linearized one-dimensional operator

$$L_f = \partial_{zz} - W''(\phi_{\mathrm{f}}), \tag{3.5}$$

which enjoys the properties outlined in Lemma A.1.

The fully dressed single-layer Ansatz has the residual

$$F(\Phi_{\mathrm{f}}) = F(\phi_{\mathrm{f}}) + \mathcal{L}(\varepsilon^2\phi_2 + \varepsilon^3 b_3) + O(\varepsilon^4), \tag{3.6}$$

where the linearization of the first variation of $\mathcal{F}$, see (1.7), about Φ_{f}, that is the second variation of $\mathcal{F}$ evaluated at Φ_{f}, takes the form

$$\mathcal{L} = (\mathcal{A} - \eta)\,\mathcal{A} - W'''(\Phi_{\mathrm{f}})(\varepsilon^2\Delta\Phi_{\mathrm{f}} - W'(\Phi_{\mathrm{f}})), \tag{3.7}$$

in terms of the "Cahn–Hilliard" linearization

$$\mathcal{A} := \frac{\delta^2 \mathcal{E}}{\delta u^2}(\Phi_{\rm f}) = -\varepsilon^2 \Delta + W''(\Phi_{\rm f}). \tag{3.8}$$

It is instructive to remark that for Φ an approximate critical point of $\mathcal{E}$, the second variation of $\mathcal{F}$ at Φ is approximately a functional mapping of the second variation of $\mathcal{E}$ at Φ. Changing to whiskered coordinates in the Laplacian and expanding the extended curvature κ according to (2.16) it is straightforward to calculate that

$$F(\phi_{\rm f}) = \varepsilon^2 \left(\kappa_0^2 \phi'' + \kappa_1 L_f(z\phi_{\rm f}')\right) + \varepsilon^3 \Big(L_f(\kappa_2 z^2 \phi_{\rm f}') + \kappa_0\kappa_1 (z\phi_{\rm f}')' + (\kappa_1 z\partial_z + \eta_2 + \Delta_s)\kappa_0 \phi_{\rm f}' \Big) + O(\epsilon^4), \tag{3.9}$$

while

$$\mathcal{L} = L_f^2 + \varepsilon\kappa_0 \left(L\partial_z + \partial_z L_f - W'''(\phi_{\rm f})\phi_{\rm f}'\right) + O(\varepsilon^2). \tag{3.10}$$

Plugging these expressions into the residual yields the expansion

$$F(\Phi_{\rm f}) = \varepsilon^2 \left(L_f^2 \phi_2 + \kappa_0^2 \phi_{\rm f}'' + \kappa_1 L_f(z\phi_{\rm f}')\right) + O(\varepsilon^3), \tag{3.11}$$

and since $\kappa_0^2 \phi_{\rm f}'' + \kappa_1 L_f(z\phi_{\rm f}') \perp_{L^2(\mathbb{R})} \ker(L_f)$, we may choose ϕ_2 to eliminate the ε^2 terms,

$$\phi_2 = L_f^{-2}(-\kappa_0^2 \phi_{\rm f}'' - \kappa_1 L_f(z\phi_{\rm f}')) = -\left(\frac{\kappa_0^2}{2} + \kappa_1\right) L_f^{-1}(z\phi_{\rm f}'), \tag{3.12}$$

where we used (A.3). With the curvature terms incorporated into ϕ_2 the residual becomes,

$$\begin{aligned} F(u) &= \epsilon^3 \Big(L_f(\kappa_0(\phi_2)_z + \kappa_2 z^2 \phi_{\rm f}') + L_f^2 b + \kappa_0 (L_f\phi_2 + \kappa_1 z\phi_{\rm f}')_z \\ &\quad + \kappa_0\kappa_1 z\phi_{\rm f}'' + (\Delta_s + \eta_2)(\kappa_0\phi_{\rm f}') - \kappa_0 W'''(\phi_{\rm f})\phi_{\rm f}'\phi_2 \Big) \\ &\quad + O(\epsilon^4). \end{aligned} \tag{3.13}$$

3.2. Single-layer interfacial dynamics

To address the geometrically driven flow of Γ we decompose u as,

$$u(x,t) = \Phi_{\rm f}(s,z,t) + v(x,t), \tag{3.14}$$

where $\Phi_{\rm f}$ is the Ansatz (3.4), which depends upon time through the hypersurface Γ and the background value $b = b_- + \varepsilon^3 b_3(t)$. The term v is the perturbation to the Ansatz which we regard as small. From the chain rule we have

$$\partial_t \Phi_{\rm f} = \phi_{\rm f}' z_t + \varepsilon^3 b_{3,t} + O(\varepsilon^2 z_t, \varepsilon^2 \kappa_t). \tag{3.15}$$

We will see below that $z_t, \kappa_t = O(\varepsilon^3)$, while $b_{3,t} = O(1)$, and the error terms are $O(\varepsilon^5)$. Putting the decomposition of u into (1.5), we obtain

$$\begin{aligned} z_t\phi_{\rm f}' + \varepsilon^3 b_{3,t} + v_t &= -\Pi_0 F(\Phi_{\rm f} + v) = -\Pi_0 F(\Phi_{\rm f}) - \mathbb{L}v \\ &\quad - \Pi_0 \mathcal{N}(v), \end{aligned} \tag{3.16}$$

where $\mathbb{L} = \Pi_0 \mathcal{L}$ and $\mathcal{N}(v)$ represents the nonlinear terms in v. While $\mathcal{L}$ is self-adjoint, $\mathbb{L}$ is not, however $\sigma(\mathbb{L}) \subset \sigma(\Pi_0 \mathcal{L} \Pi_0) \cup \{0\}$ is real, and moreover $\sigma(\Pi_0 \mathcal{L} \Pi_0)$ interleaves $\sigma(\mathcal{L})$, so that the spectral set of $\mathcal{L}$ controls that of $\mathbb{L}$, see [34] for details (see Fig. 3.1).

The adjoint operator $\mathbb{L}^\dagger = \mathcal{L}\Pi_0$ has a kernel spanned by the constant function $\Psi_0^\dagger \equiv 1$. Extending the results of [33], it has been shown in [35] that the spectrum of $-\mathcal{L}$ is bounded above by a constant of $O\left(\varepsilon^2 \|\kappa_0\|^2_{L^\infty(\Gamma)}, \varepsilon^4 \eta_2^2\right)$. More significantly, there exists $\nu > 0$ for which the adjoint eigenspace corresponding to eigenvalues of $-\mathbb{L}$ which are greater than $-\nu\varepsilon$ is spanned by functions

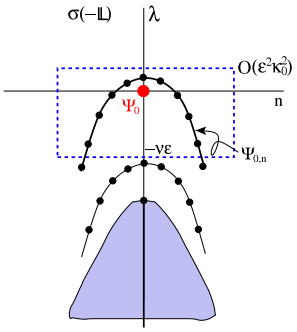

Fig. 3.1. A cartoon representation of spectrum of the linear operator, $-\mathbb{L}$, of the ZMFCH about a single-layer dressed interface. The eigenvalues (all real) are plotted against the transverse index n, with the associated eigenfunctions Ψ_0 and $\Psi_{0,n}$ indicated. The blue box indicates the eigenspace employed in the spectral projection. The interface curvatures increase the translational eigenvalues associated to $\{\Psi_{0,n}\}$ by $O(\varepsilon^2\kappa_0^2)$.

$\{\Psi_{0,n}^\dagger | 1 \le n \le N_\varepsilon\}$ with a separated variables decomposition

$$\Psi_{0,n}^\dagger(s,z) = \varepsilon^{-\frac{1}{2}} \phi_{\rm f}'(z)\Theta_n(s) + \Psi_{0,n}^\perp(s,z). \tag{3.17}$$

The perturbations $\Psi_{0,n}^\perp$ are orthogonal to $\phi_{\rm f}'$ on each whisker and are $O(\varepsilon)$ in $L^2(\Omega)$, while the scaling gives the leading order term an $L^2(\Omega)$ norm of 1 with Θ_n independent of ε. Moreover the $\{\Theta_n\}_{n=0}^{N_\varepsilon}$ form an approximate basis of $L^2(\Gamma)$, in the sense that any function f which is orthogonal to this set in $L^2(\Gamma)$ satisfies the inequality

$$\|f\|_{L^2(\Gamma)} \le \varepsilon c \|\Delta_s f\|_{L^2(\Gamma)}, \tag{3.18}$$

for a constant $c > 0$ which depends only upon ν and Γ. To render the decomposition (3.14) unique, we impose the non-degeneracy conditions

$$v \perp \{\Psi_0^\dagger\} \cup \{\Psi_{0,j}^\dagger | 1 \le j \le N_\varepsilon\}. \tag{3.19}$$

These conditions make the semigroup generated by $\mathbb{L}$ uniformly contractive on v. In particular, so long as the flow leaves Γ within the admissible class of interfaces, we assume that v remains the same size as the residual, namely $O(\varepsilon^3)$ in $L^2(\Omega)$, and that the nonlinear terms $\mathcal{N}(v)$ are yet higher order and hence negligible, see [36,37] for rigorous treatments.

To obtain the normal front velocity we project (3.16) onto the eigenspace spanned by $\{\Psi_{0,j}^\dagger\}_{j=1}^{N_\varepsilon}$. The linear terms in v and v_t drop out due to (3.19). Neglecting the nonlinear terms in v, the remaining terms are localized on Γ, and we may change to the whiskered coordinate system. Using the Jacobian expansion (2.13) we obtain the leading order expression

$$\begin{aligned} &\int_\Gamma \left(\|\phi_{\rm f}'\|_2^2 z_t + \varepsilon^3 [\![\phi_{\rm f}]\!] b_{3,t}\right) \Theta_n(s)\, {\rm d}s \\ &\quad = -\int_\Gamma \Theta_n(s) (\Pi_0 F(\Phi), \phi_{\rm f}')_2\, {\rm d}s. \end{aligned} \tag{3.20}$$

The integrands of (3.20) depend upon s only through the curvatures of Γ, and for admissible interfaces these are smooth functions. Thus it follows from the approximate basis property of the $\Theta_j's$ that we may equate the two integrands as $L^2(\Gamma)$ functions at leading order,

$$z_t = -\frac{(F(\Phi_{\rm f}), \phi_{\rm f}')_2}{\|\phi_{\rm f}'\|_2^2} + \left(\langle F(\Phi_{\rm f})\rangle_\Omega - \varepsilon^3 b_{3,t}\right) \frac{[\![\phi_{\rm f}]\!]}{\|\phi_{\rm f}'\|_2^2}. \tag{3.21}$$

To simplify (3.21) we take the $L^2(\mathbb{R})$ inner product of (3.13) with ϕ' and integrate by parts to cancel the $\kappa_0\kappa_1$ terms. We obtain

$$\begin{aligned} (F(\Phi_{\rm f}), \phi_{\rm f}')_2 &= \epsilon^3 \Big[-\kappa_0 (L_f\phi_2, \phi_{\rm f}'') + (\Delta_s + \eta_2)(\kappa_0) \|\phi_{\rm f}'\|_2^2 \\ &\quad - \kappa_0 (W'''(\phi_{\rm f})(\phi_{\rm f}')^2, \phi_2) \Big] + O(\epsilon^4). \end{aligned} \tag{3.22}$$

Using the definition (3.12) of ϕ_2 we evaluate

$$(L_f\phi_2, \phi_f'') = -\left(\frac{\kappa_0^2}{2}+\kappa_1\right)\left(z\phi_f', \phi_f''\right)_{L^2} = \frac{1}{2}\left(\frac{\kappa_0^2}{2}+\kappa_1\right)\|\phi_f'\|_2^2, \tag{3.23}$$

while (3.12) and (A.2) show that

$$(W'''(\phi_f)(\phi_f')^2, \phi_2) = -\left(\frac{\kappa_0^2}{2}+\kappa_1\right)\left(L_f\phi_f'', L_f^{-1}z\phi_f'\right)_2 = \frac{1}{2}\left(\frac{\kappa_0^2}{2}+\kappa_1\right)\|\phi_f'\|_2^2. \tag{3.24}$$

Combining these results gives the leading order expression

$$(F(\Phi_f), \phi_f') = \epsilon^3\|\phi_f'\|_{L^2}^2\left((\Delta_s+\eta_2)\kappa_0 - \left(\frac{\kappa_0^3}{2}+\kappa_0\kappa_1\right)\right) + O(\epsilon^4), \tag{3.25}$$

and introducing the scaled normal front velocity $\mathbf{V}_n = -\varepsilon^{-3}z_t$, we rewrite (3.21) as

$$\mathbf{V}_n = \left[(\Delta_s+\eta_2)\kappa_0 - \left(\frac{\kappa_0^3}{2}+\kappa_0\kappa_1\right)\right] - \left(\varepsilon^{-3}\langle F(\Phi_f)\rangle_\Omega - b_{3,t}\right)\frac{[\![\phi_f]\!]}{\|\phi_f'\|_2^2}. \tag{3.26}$$

To evaluate $\langle F(\Phi_f)\rangle_\Omega$ we return to (3.13) and observe that all terms except those involving the background perturbation, b_3, are localized on Γ. We integrate over Ω and change to the whiskered variables for the localized terms. So long as $|\Gamma| = O(1) \ll \varepsilon^{-1}$, the extra factor of ε that the localized terms acquire from the Jacobian renders them lower order than the far-field terms. At the leading order we have

$$\langle F(\Phi_f)\rangle_\Omega = \frac{\varepsilon^3}{|\Omega|}\int_\Omega L_f^2 b_3\,dx + O(\varepsilon^4) = \frac{\varepsilon^3 b_3}{|\Omega|}\int_\Omega \left(W''(\phi_f)\right)^2\,dx + O(\varepsilon^4) = \varepsilon^3 b_3\mu_0^2 + O(\varepsilon^4), \tag{3.27}$$

where we have introduced $\mu_0^2 = \frac{|\Omega_-|\mu_-^2+|\Omega_+|\mu_+^2}{|\Omega|} > 0$. Combining (3.26) with (3.27) we obtain

$$\mathbf{V}_n = \left(\Delta_s+\eta_2-\frac{\kappa_0^2}{2}-\kappa_1\right)\kappa_0 + \frac{[\![\phi_f]\!]}{\|\phi_f'\|_2^2}\left(b_{3,t}-\mu_0^2 b_3\right) + O(\varepsilon). \tag{3.28}$$

The evolution of the background state is determined from the total mass conservation. Projecting (3.16) onto $\Psi_0^\dagger = 1$, the right-hand side is identically zero and we obtain

$$b_{3,t} = -\frac{\varepsilon^{-3}}{|\Omega|}\int_\Omega z_t\phi_f'\,dx = -\varepsilon^{-2}\frac{[\![\phi_f]\!]}{|\Omega|}\int_\Gamma z_t\,ds = \varepsilon\frac{[\![\phi_f]\!]}{|\Omega|}\int_\Gamma \mathbf{V}_n\,ds. \tag{3.29}$$

Substituting the normal velocity, (3.28), into this expressing and dropping the lower order terms yields an ordinary differential equation for b_3,

$$b_{3,t} + \varepsilon\frac{\mu_0^2[\![\phi_f]\!]^2|\Gamma|}{\|\phi_f'\|_2^2|\Omega|}b_3 = \varepsilon\frac{[\![\phi_f]\!]}{|\Omega|}\int_\Gamma\left(\Delta_s+\eta_2-\frac{\kappa_0^2}{2}-\kappa_1\right)\kappa_0\,ds + O(\varepsilon^2). \tag{3.30}$$

This equation relaxes on a *fast*, $t = O(\varepsilon^{-1})$, time-scale to a stable equilibrium determined by a Γ-averaged value of the front curvatures

$$b_3 = \frac{\|\phi_f'\|_2^2}{\mu_0^2[\![\phi_f]\!]|\Gamma|}\int_\Gamma\left(\Delta_s+\eta_2-\frac{\kappa_0^2}{2}-\kappa_1\right)\kappa_0\,ds + O(\varepsilon). \tag{3.31}$$

In turn the curvatures evolve on a *slow* $t = O(\varepsilon^{-3})$ time scale adiabatically driving the equilibrium value of b_3. On this longer time-scale, the background evolution becomes $b_{3,t} = O(\varepsilon^3)$, which may then be neglected in (3.28). On closer inspection, one observes that the equilibrium value of the background is exactly the average value of the normal velocity over the surface Γ. More specifically, the fast–slow system (3.28)–(3.30) yields an effective evolution which may be succinctly written as

$$\mathbf{V}_n = \Pi_{0,\Gamma}\left(\Delta_s+\eta_2-\frac{\kappa_0^2}{2}-\kappa_1\right)\kappa_0 + O(\varepsilon), \tag{3.32}$$

where $\Pi_{0,\Gamma}$ denotes the zero-mass projection over the interface Γ.

3.3. Two-dimensional results

In two space-dimensions the mean curvature is the unique curvature, which determines the shape of the hypersurface up to rigid body rotations. We can relate the curvature back to the z variable through the equalities $\nu = \varepsilon\nabla_x z$ and $\kappa = \nabla_x\cdot\nu$. Introducing the slow time $\tau = \varepsilon^4 t$, we have

$$\kappa_\tau = \varepsilon^3\nabla_x\cdot\nabla_x z_t = -\Delta_s\mathbf{V}_n. \tag{3.33}$$

However, in two dimensions (2.15) reduces to

$$\kappa(s,z,\tau) = \frac{\kappa_0(s,\tau)}{1+\varepsilon z\kappa_0(s,\tau)}, \tag{3.34}$$

where κ_0 is the curvature. In particular $\kappa_1 = -\kappa_0^2$, and the normal velocity reduces to

$$\mathbf{V}_n = \Pi_{0,\Gamma}\left(\partial_s^2+\eta_2+\frac{\kappa_0^2}{2}\right)\kappa_0 + O(\varepsilon). \tag{3.35}$$

Taking the derivative of (3.34) with respect to τ and introducing $z_\tau = -\varepsilon^{-1}\mathbf{V}_n$ we find

$$\kappa_\tau = \frac{\partial_\tau\kappa_0(1+\varepsilon z\kappa_0) - \kappa_0^2\varepsilon z_\tau - \varepsilon z\kappa_0\partial_\tau\kappa_0}{(1+\varepsilon\kappa_0 z)^2} = \partial_\tau\kappa_0 + \kappa_0^2\mathbf{V}_n + O(\varepsilon), \tag{3.36}$$

and the leading order terms in (3.33) become

$$\partial_\tau\kappa_0 = -\left(\partial_s^2+\kappa_0^2\right)\mathbf{V}_n(\kappa_0). \tag{3.37}$$

In the context of the ZMFCH equation, the explicit normal velocity of a single-layer interface takes the form

$$\partial_\tau\kappa_0 = -\left(\partial_s^2+\kappa_0^2\right)\Pi_{0,\Gamma}\left((\partial_s^2+\eta_2)\kappa_0+\frac{1}{2}\kappa_0^3\right). \tag{3.38}$$

The result above assumes that s is arc-length along the curve, however as the normal velocity stretches the curve, the arc-length must be re-parameterized. We identify an arbitrary point on the curve as $s = 0$, and maintain this label through its evolution by normal velocity. The re-parameterization incorporates a convective term which accounts for the splaying of the lines of constant s. With this modification the $\mathbb{R}^2$ evolution equation becomes

$$\partial_\tau\kappa_0 + \left(\int_0^s \mathbf{V}_n\kappa_0(s)\,ds\right)\partial_s\kappa_0 = -\left(\partial_s^2+\kappa_0^2\right)\Pi_{0,\Gamma}\left((\partial_s^2+\eta_2)\kappa_0+\frac{1}{2}\kappa_0^3\right). \tag{3.39}$$

It follows immediately from (3.39) that a circular interface of any radius is stationary. Indeed the curvature is independent of s and the zero-mass projection $\Pi_{0,\Gamma}$ annihilates the constant residual on the right-hand side. On the other hand, if Γ consists of two well-separated circles of differing radius, then the larger curvature circle (smaller radius) will shrink in curvature (grow in radius) while the smaller curvature circle (larger radius) will grow in curvature (shrink in radius). Barring instability of the circular shape, the two circles will converge to a common radius. However, an analysis of circular curves shows that if their radius is sufficiently large, then they are linearly unstable to non-radial perturbations. Indeed, consider a surface Γ whose curvature is a small, zero mass perturbation from a constant value, $\kappa_0 = \overline{\kappa}_0 + v(s,\tau)$ with $\|v\|_{L^\infty(\Gamma)} \ll 1$. The linear evolution for v is given by

$$\partial_\tau v = -\left(\partial_s^2 + \overline{\kappa}_0^2\right)\left(\partial_s^2 + \eta_2 + \frac{3}{2}\overline{\kappa}_0^2\right) v, \tag{3.40}$$

with the zero mass projection and the convective re-parameterization both contributing at a nonlinear level in v. On a circle with curvature $\overline{\kappa}_0$, the eigenfunctions of the linear operator on the right-hand side of (3.40) are of the form $\psi_n(s) = \mathrm{e}^{\mathrm{i}\xi_n s}$. The constraints that the perturbation correspond to a closed curve, and be $2\pi\overline{\kappa}_0^{-1}$-periodic, leaves the spatial frequencies $\xi_n = n\overline{\kappa}_0$, for $n = \pm 2, \pm 3, \ldots$. The associated eigenvalues of this operator are given by

$$\mu_n = -\overline{\kappa}_0^4\left(-n^2+1\right)\left(-n^2 + \frac{\eta_2}{\overline{\kappa}_0^2} + \frac{3}{2}\right). \tag{3.41}$$

The most unstable eigenvalues, $\mu_{\pm 2}$, are positive so long as the functionalization constant η_2 is sufficiently large compared to the curvature,

$$\eta_2 > \frac{\overline{\kappa}_0^2}{2}. \tag{3.42}$$

The resultant instability is manifest as an "antipodal" stretching of the near-circular interface. Conversely, circles with sufficiently small radius are linearly stable under the evolution. We remark that the rigid body translation of the curve is not detectable through the curvature formation, and constitute neutral modes in the linear stability.

4. The bi-layer dressing

For the single-layer dressing, there was a self-evident class of 1D critical points available. For a bi-layer dressing, we first re-examine the mass-constrained critical points of (1.4) which satisfy the equation

$$\Pi_0 \frac{\delta \mathcal{F}}{\delta u}(u) = 0. \tag{4.1}$$

This is a fourth order differential operator coupled to a rank-one projection, a combination whose rich structure provides for the existence of *families* of equilibria. We construct a class of approximate 1D critical points that correspond to interfacial bi-layers with a homoclinic or pulse-like profile in their transverse cross-section. To accomplish this construction we unfold the saddle–saddle connection of the single-layer or heteroclinic solutions by introducing parameters corresponding to *neutral modes* of the energy. We begin by observing that the kernel of Π_0 is comprised of the spatial constants on Ω, so if the shifted functional $\mathcal{J}$ satisfies

$$\frac{\delta \mathcal{J}}{\delta u} = \frac{\delta \mathcal{F}}{\delta u} + c, \tag{4.2}$$

for some constant c, then u will satisfy (4.1) for $\mathcal{J}$ exactly when it does for $\mathcal{F}$. The first parameter we introduce is the background state b of the homoclinic pulse profile, which is dual to the kernel of Π_0. To proceed, after an integration by parts we may write the functionalized energy as

$$\mathcal{F}(u) = \int_\Omega \frac{1}{2}\varepsilon^4(\Delta u)^2 + \varepsilon^2 f_1(u)|\nabla u|^2 + f_2(u)\,\mathrm{d}x, \tag{4.3}$$

where we have introduced

$$f_1(u) = W''(u) - \frac{\eta}{2}, \tag{4.4}$$

$$f_2(u) = \frac{1}{2}(W'(u))^2 - \eta W(u). \tag{4.5}$$

We modify the potential f_2 to have a double zero at $u = b$,

$$f_3(u) = f_2(u) - f_2'(b)(u-b) - f_2(b), \tag{4.6}$$

and define the shifted energy

$$\mathcal{J}(u) = \int_\Omega \frac{1}{2}\varepsilon^4(\Delta u)^2 + \varepsilon^2 f_1(u)|\nabla u|^2 + f_3(u)\,\mathrm{d}x, \tag{4.7}$$

which satisfies (4.2) for $c = -f_2'(b)$. We rewrite the shifted energy in terms of the potential

$$G_0(u) \equiv \int_b^u \int_{s_1=b}^{s_2} f_1(s_1)\,\mathrm{d}s_1\,\mathrm{d}s_2 = W_T(u;b) - \frac{\eta}{4}(u-b)^2, \tag{4.8}$$

where $W_T(u;b) = W(u) - W(b) - W'(b)(u-b)$ is the result of shifting the double zero of W at b_- to b by subtracting the appropriate Taylor polynomial. Integrating by parts on f_1 in (4.7) and completing the square we obtain

$$\mathcal{J}(u) = \int_\Omega \frac{1}{2}\left(\varepsilon^2\Delta u - G_0'(u)\right)^2 + p(u)\,\mathrm{d}x, \tag{4.9}$$

where $p(u) = f_3(u) - \frac{1}{2}\left(G_0'(u)\right)^2$.

Lemma 4.1. *The potential p takes the form*

$$p(u) = \left(W_T'(u) - W''(b)(u-b)\right)W'(b) - \eta W_T(u) + \frac{\eta}{2}\left(W_T'(u) - \frac{\eta}{4}(u-b)\right)(u-b), \tag{4.10}$$

with a double zero at $u = b$. With the scaling $b = b_- + \varepsilon^2 b_2$ and $\eta = \varepsilon^2\eta_2$ then $p(u) = \varepsilon^2 p_2(u)$ where

$$p_2(u) = \overbrace{\mu_-\left(W'(u) - W'(b) - \mu_-(u-b)\right)}^{p_{20}(u)} b_2 + \overbrace{\left(\frac{1}{2}W'(u)(u-b) - W(u) + W(b)\right)}^{p_{21}(u)}\eta_2 + O(\varepsilon), \tag{4.11}$$

in $L^\infty([b,-b])$, and $\mu_- = W''(b_-)$. Moreover, if $uW'''(u) > 0$, then both p_{20} and p_{21} are non-positive on $[b,-b]$, and zero at $z = b$.

Proof. The expression (4.10) follows from the definitions of f_3 and G_0. The expression (4.11) follows from an expansion of W' and W about $-b_-$. To see that p_{20} is non-positive on $[-b,b]$, observe that $p_{20}(b) = 0$ while $p_{20}'(u) = W''(u) - W''(b_-)$. From the assumption on W''' we see that W'' has a global minima at $u = 0$ and is strictly decreasing on $[b,0]$, hence $p_{20}' < 0$ on $[b,0]$, and by symmetry on $[0,-b]$, so that p_{20} is decreasing on $[b,-b]$. Turning to p_{21} we observe that $p_{21}(\pm b) = 0$ with $p_{21}(-b) > 0$ and p_{21} having a third-order zero at $u = b$ with $p_{21}(u) < 0$ for $0 < u - b \ll 1$. Observing that $p_{21}'' = W'''(u)(u-b)$, is zero at $u = b$ and $u = 0$, we see that p_{21}' can have at most one zero in $(b,-b)$, and hence p_{21} has exactly one zero on (b,∞), which must be the zero at $u = -b$. □

4.1. The detuning parameter and reduction to 2nd order

To break the degeneracy of the saddle–saddle connection of the heteroclinic associated to the potential W we introduce a "tilt" parameter α which tunes the shape of the potential,

$$G(u;\alpha,b) = G_0(u;b) - \varepsilon\alpha g(u;b). \tag{4.12}$$

The optimal choice for the perturbation g will be made explicit below. With this notation $\mathcal{J}$ can be written

$$\mathcal{J}(u;\alpha,b) = \int_\Omega \frac{1}{2}\left(\varepsilon^2\Delta u - G'(u) - \varepsilon\alpha g'(u)\right)^2 + p(u)\,\mathrm{d}x, \tag{4.13}$$

so that (1.5) has the equivalent formulation,

$$u_t = -\Pi_0\frac{\delta\mathcal{J}}{\delta u} = -\Pi_0\overbrace{\left(\left(\varepsilon^2\Delta - G''(u) - \varepsilon\alpha g''(u)\right)\left(\varepsilon^2\Delta u - G'(u) - \varepsilon\alpha g'(u)\right) + p'(u)\right)}^{S(u)}. \tag{4.14}$$

We wish to define the leading order bi-layer solution, $\phi = \phi(z;\alpha,b)$, as the unique solution of the 1D, scaled equation

$$\phi'' = G'(\phi), \tag{4.15}$$

which is homoclinic to b and symmetric about $z = 0$. The existence of ϕ requires that the potential G has a double zero at $u = b$ and a second, transverse zero to the right of b. Accordingly we impose the constraints $g(b) = g'(b) = 0$, as well as $g > 0$ on (b,∞) with $g(s) \ll G(s)$ for s sufficiently large. For such g the following lemma holds.

Lemma 4.2. *In the scaling $b = b_- + \varepsilon^2 b_2$ and $\eta = \varepsilon^2\eta_2$ there exists a smooth function*

$$\alpha_*(b) = -\frac{\varepsilon}{g(b_+)}\left(\mu_- b_2(b_+ - b_-) + \frac{\eta_2}{4}(b_+ - b_-)^2\right) + O(\varepsilon^2), \tag{4.16}$$

for which $G(\cdot;\alpha_*(b),b)$ has a double zero at $u = \phi_m^*(b)$. For $\alpha > \alpha_*$, this double zero breaks into two zeros, the smaller of which takes the form

$$\phi_m(\alpha,b) = b_+ - \sqrt{\frac{2\varepsilon\alpha g(b_+)}{\mu_+}} + O\left(\varepsilon^{\frac{3}{2}}\right). \tag{4.17}$$

In particular, the value $\phi_m(\alpha)$ is the maximum of ϕ over $z \in \mathbb{R}$. and

$$p_2(\phi_m) = -\mu_+^2(b_+ - b_-)b_2 - \sqrt{\frac{2\alpha g(b_+)}{\mu_+}}\left(\mu_-(\mu_+ - \mu_-)b_2 + \frac{\mu_+}{2}(b_+ - b_-)\eta_2\right)\varepsilon^{\frac{1}{2}} + O(\varepsilon), \tag{4.18}$$

which is positive so long as $b_2 < 0$.

Proof. The expression (4.17) follows from a Taylor expansion of G near b_+, and (4.18) results from substitution of (4.17) into (4.11). □

Linearizing the differential equation (4.15) about ϕ yields the operator

$$L = \partial_{zz} - G''(\phi), \tag{4.19}$$

whose point spectrum and eigenfunctions play a crucial role in the geometric surface evolution. We choose g, satisfying the properties above, to simplify the analysis. The 1D version of the full critical point equation, (4.1) is a fourth-order ODE whose exponential dichotomies contain complex eigenvalues with $O(\varepsilon^2)$ imaginary parts. As a consequence, an exact homoclinic solution will manifest oscillations of $O(\varepsilon^2)$ magnitude at spatial infinity, which is impossible for homoclinic solutions of second order equations. An optimal choice of g will yield a second order Eq. (4.15) whose homoclinic solution is the correct bi-layer Ansatz to $O(\varepsilon^2)$. Achieving this requires that g satisfies $Lg'(\phi) = O(\varepsilon)$. The choice

$$g(u;b) \equiv \int_b^u \sqrt{W_s(t;b)}\,\mathrm{d}t, \tag{4.20}$$

where $W_s(u;b) = W(u - \varepsilon^2 b_2)$ is a shifting of the double well, realizes this goal by rendering $g'(\phi)$ asymptotically proportional to the ground state eigenfunction of L which bifurcates from zero when $\alpha > \alpha_*$. This is the second neutral mode we seek.

Lemma 4.3. *Let g be as in (4.20) with $\varepsilon \ll 1$. Then there exists $\nu_0 > 0$, independent of ε, such that the spectrum of the linear operator L given in (4.19) consists of two point eigenvalues*

$$\sigma_p(L) = \{\lambda_1 = 0, \lambda_0(\alpha,b)\}, \tag{4.21}$$

and a remainder contained in $(-\infty,-\nu_0]$. The ground state eigenvalue is given by the formula

$$\lambda_0 = \varepsilon\frac{4\alpha\gamma_0}{\|\phi'\|_2^2} + O\left(\varepsilon^2\right), \tag{4.22}$$

where

$$\gamma_0 \equiv -\left(g'''(\phi)g(\phi), g'(\phi)\right)_2 = \sqrt{\mu_+}g(b_+) + O(\sqrt{\varepsilon}) > 0. \tag{4.23}$$

The corresponding normalized eigenfunctions take the form

$$\psi_1 = \frac{\phi'}{\|\phi'\|_2}, \tag{4.24}$$

$$\psi_0 = \frac{g'(\phi)}{\|g'(\phi)\|_2} + O(\varepsilon), \tag{4.25}$$

with the equality on ψ_0 holding in L^2. Moreover we may relate $g'(\phi)$ to the translational eigenvalue

$$g'(\phi) = \frac{1}{\sqrt{2}}|\phi'| + O(\sqrt{\varepsilon}), \tag{4.26}$$

in the L^1 norm.

Proof. The operator L is a self-adjoint, 2nd-order, Sturm–Liouville operator and its spectrum is real. It is well known that linearizing about two well-separated front solutions produces a point spectrum consisting of two localized copies of the spectrum of a single front. Since ϕ_f has a simple eigenvalue at $\lambda = 0$ with the remainder of its spectrum to the left of $-\nu_0$, it remains to determine the location of the two small eigenvalues of L. We first take the z derivative of (4.15) which shows, from the translational symmetry, that ϕ' is in the kernel of L. This eigenvalue has one node so the Sturm–Liouville theory implies that the ground state eigenvalue, λ_0, must be positive.

To develop an expansion for λ_0 and the ground-state $\psi_0 > 0$, we first re-write the potential G as

$$G(s) = \left(g'(s)\right)^2 - \varepsilon\alpha g(s) + \varepsilon^2 h(s), \tag{4.27}$$

where the higher order term

$$h(s) = \varepsilon^{-2}(W_T(s) - W_s(s)) - \frac{\eta_2}{4}(s-b)^2 = \left(W'(s) - \mu_-(s-b)\right)b_2 - \frac{\eta_2}{4}(u-b)^2 + O(\varepsilon), \tag{4.28}$$

has a double zero at $s = b$, is $O(1)$ over the range of ϕ and is smooth. The function g is only $\mathcal{C}^1$ with discontinuities in its second derivative at $s = b, b_+ - \varepsilon^2 b_2$. However g is piece-wise $\mathcal{C}^\infty$, and

is $\mathcal{C}^\infty$ on the range of ϕ, since $\phi_m(b) < b_+ - \varepsilon^2 b_2$. Applying L to $g'(\phi)$ and using (4.15) and its first integral

$$\frac{1}{2}\left(\phi'\right)^2 = G(\phi), \tag{4.29}$$

to eliminate derivatives of ϕ, we obtain

$$Lg'(\phi) = 2g'''(\phi)G(\phi) + g''(\phi)G'(\phi) - G''(\phi)g'(\phi). \tag{4.30}$$

Taking derivatives of (4.27) with respect to s we may eliminate G for g and h and their derivatives. The leading order terms cancel, yielding

$$Lg'(\phi) = -2\varepsilon\alpha g'''(\phi)g(\phi) + \varepsilon^2 r(\phi), \tag{4.31}$$

where the second order term

$$r(s) = 2g'''h + g''h' - g'h'', \tag{4.32}$$

is zero at $s = b$ and hence $r(\phi)$ is $O(1)$ in L^2. Since the right-hand side of (4.31) is even, it is orthogonal to the kernel of L and we may invert, yielding

$$g'(\phi) = -\frac{2\varepsilon\alpha\left(g'''(\phi)g(\phi) + \varepsilon r(\phi), \psi_0\right)_2}{\lambda_0}\psi_0 + \varepsilon g^\perp, \tag{4.33}$$

in L^2, where $g^\perp \perp \psi_0$ is $O(1)$. Taking the L^2 norm of both sides of (4.33), we deduce that $\|g'(\phi)\|_2 = O(1)$ since ϕ ranges from b to ϕ_m with $O(1)$ derivatives. From this we may infer that $\lambda_0 = O(\varepsilon)$, which further yields the asymptotic expression

$$\lambda_0 = \frac{2\varepsilon\alpha|\left(g'''(\phi)g(\phi), \psi_0\right)_2|}{\|g'(\phi)\|_2} + O(\varepsilon^2). \tag{4.34}$$

Dividing both sides of (4.33) by their L^2 norms yields (4.25), and using this to substitute for ψ_0 in (4.34) yields (4.22) with $\gamma_0 = -\left(g'''(\phi)g(\phi), g'(\phi)\right)_2$. Using (4.27) and (4.29) we may isolate $g'(\phi)$,

$$g'(\phi) = \sqrt{\frac{1}{2}|\phi'|^2 + \varepsilon\alpha g(\phi) - \varepsilon^2 h(s)}. \tag{4.35}$$

Expanding this expression yields (4.26), except for a neighborhood of $z = 0$ where $\phi'(z) = \phi''(0)z + O(z^3)$ where $\phi''(0) = G'(\phi_m) = O(\sqrt{\varepsilon})$. These estimates yield the $O(\sqrt{\varepsilon})$ error bound in (4.26). To simplify the expression for γ_0 we use (4.26) to write

$$\begin{aligned}\gamma_0 &= -\frac{1}{\sqrt{2}}\int_{\mathbb{R}} g'''(\phi)g(\phi)|\phi'|\,dz + O(\sqrt{\varepsilon})\\ &= \sqrt{2}\int_0^\infty \partial_z\left(g''(\phi)\right)g(\phi)\,dz + O(\sqrt{\varepsilon}),\\ &= -\frac{1}{\sqrt{2}}\int_0^\infty \partial_z(g'(\phi))^2\,dz + \sqrt{2}(g''(b)g(b)\\ &\quad - g''(\phi_m)g(\phi_m)).\end{aligned} \tag{4.36}$$

However $g'(b) = 0$ and $g'(\phi_m) = O(\sqrt{\varepsilon})$ so its square is $O(\varepsilon)$. Similarly, $g(b) = 0$, and the expression reduces to

$$\gamma_0 = -\sqrt{2}g''(\phi_m)g(b_+) + O(\sqrt{\varepsilon}). \tag{4.37}$$

Finally,

$$g''(\phi_m) = \frac{W_s'(\phi_m)}{2\sqrt{W_s(\phi_m)}} = -\sqrt{\frac{\mu_+}{2}} + O(\sqrt{\varepsilon}), \tag{4.38}$$

and we recover (4.23). □

For $i = 0$ and 1 we introduce the spectral projection π_i associated to the eigenvector ψ_i,

$$\pi_i f = (f, \psi_i)_2\psi_i, \tag{4.39}$$

and their sum $\pi = \pi_0 + \pi_1$, and its complement $\tilde{\pi} = I - \pi$.

Lemma 4.4. *The partial derivatives of the pulse with respect to the detuning parameter takes the form*

$$\partial_\alpha\phi = -\rho_\alpha\psi_0 + \varepsilon^2\phi_\alpha^\perp, \tag{4.40}$$

where $\rho_\alpha = \rho_{\alpha_0}/(\alpha - \alpha_*) + O(\varepsilon)$ *with*

$$\rho_{\alpha,0} = \frac{\|\phi'\|_2^3}{4\sqrt{2}\gamma_0} > 0, \tag{4.41}$$

and

$$\phi_\alpha^\perp = -L^{-1}\tilde{\pi}g'(\phi), \tag{4.42}$$

is $O(1)$ in L^2. The partial derivative of the pulse with respect to the background b takes the form

$$\partial_b\phi = -\varepsilon^{-1}\rho_b\psi_0 + 1 + \phi_b^\perp, \tag{4.43}$$

where

$$\rho_b = \frac{\mu_-\|\phi'\|_2^2}{4\alpha\gamma_0}\overline{\psi_0} + O(\varepsilon) > 01 \tag{4.44}$$

and $\|\phi_b^\perp\|_2 = O(1)$, and is orthogonal to ψ_0 and ψ_1.

Proof. Taking the α partial derivative of (4.15) yields the equality

$$L\partial_\alpha\phi = -\varepsilon g'(\phi) = -\varepsilon(g'(\phi), \psi_0)_2\psi_0 - \varepsilon\tilde{\pi}g'(\phi). \tag{4.45}$$

Inverting L yields

$$\partial_\alpha\phi = -\varepsilon\frac{(g'(\phi), \psi_0)_2}{\lambda_0}\psi_0 - \varepsilon L^{-1}\tilde{\pi}g'(\phi), \tag{4.46}$$

using (4.25) and (4.22) to replace ψ_0 and λ_0, and observing that $\tilde{\pi}g'(\phi) = O(\varepsilon)$ yields (4.40).

From (4.12) we observe that

$$\begin{aligned}\partial_b G'(u) &= -W''(b) + \varepsilon\alpha g''(u) + \varepsilon^2\frac{\eta}{2} = -G_0''(b)\\ &\quad + \varepsilon\alpha g''(u),\end{aligned} \tag{4.47}$$

so that taking ∂_b of (4.15) yields

$$L\partial_b\phi = -G_0''(b) + \varepsilon\alpha g''(\phi) \tag{4.48}$$

which can be written in terms of $L^2(\mathbb{R})$ functions as

$$\begin{aligned}L(\partial_b\phi - 1) &= G''(\phi) - G_0''(b) + \varepsilon\alpha g''(\phi)\\ &= G_0''(\phi) - G_0''(b).\end{aligned} \tag{4.49}$$

Projecting onto ψ_0 and its complement and inverting we obtain

$$\partial_b\phi - 1 = \varepsilon^{-1}\rho_b\psi_0 + \phi_b^\perp, \tag{4.50}$$

where

$$\begin{aligned}-\rho_b &= \varepsilon(\partial_b\phi - 1, \psi_0)_2 = \frac{\varepsilon}{\lambda_0}(L\partial_b\phi, \psi_0)_2 - \varepsilon\overline{\psi_0}\\ &= -\frac{\varepsilon}{\lambda_0}G_0''(b)\overline{\psi_0} + O(\varepsilon).\end{aligned} \tag{4.51}$$

However, $G''(b) = W''(b_-) + O(\varepsilon) = \mu_- + O(\varepsilon)$, and replacing λ_0 with (4.22) yields (4.43) and (4.44) with

$$\phi_b^\perp = L^{-1}\tilde{\pi}\left(G_0''(\phi) - G_0''(b)\right). \quad \square \tag{4.52}$$

4.2. Construction of the homoclinic profile

Prior to constructing the fully dressed Ansatz, we first consider a formal construction of an homoclinic solution of the fourth-order problem in one space dimension. This requires a consistency condition relating α and b, which is recovered in Section 5.1 as an equilibrium solution of the dynamics. This construction requires tuning α as a function of the background state b. We recall the scalings $b = b_- + \varepsilon^2 b_2$, $\eta = \varepsilon^2\eta_2$, and $p = \varepsilon^2 p_2$ and determine α for which we can construct $\Phi_0 = \Phi_0(z; b, \varepsilon)$ that solves

$$\begin{aligned} S(\Phi_0) &= \left(\partial_z^2 - G''(\Phi_0) - \varepsilon\alpha g''(\Phi_0)\right) \\ &\quad\times \left(\partial_z^2\Phi_0 - G'(\Phi_0) - \varepsilon\alpha g'(\Phi_0)\right) \\ &\quad + \varepsilon^2 p_2'(\Phi_0) = 0. \end{aligned} \tag{4.53}$$

We write $\Phi_0 = \phi + \varepsilon\phi_1 + \cdots$ where ϕ_1 is orthogonal to ψ_0. We substitute this ansatz into (4.53) and expand in ε. At the leading order we find

$$\begin{aligned} S(\Phi_0) &= \left(L - \varepsilon G'''(\phi)\phi_1 - \varepsilon\alpha g''(\phi)\right) \\ &\quad\times \left(\varepsilon L\phi_1 - \varepsilon\alpha g'(\phi) + \varepsilon^2 A_2\right) + \varepsilon^2 p_2'(\phi) + O\left(\varepsilon^3\right), \end{aligned} \tag{4.54}$$

where we will see that the form of the second order term, A_2, in the Cahn–Hilliard remainder is not relevant at the leading order. Solving $S(\Phi_0) = 0$ for ϕ_1 at the leading order we find

$$\begin{aligned} L^2\phi_1 &= L\left(\alpha g'(\phi) - \varepsilon A_2\right) - \varepsilon p_2'(\phi) + \varepsilon\left(G'''(\phi)\phi_1 + \alpha g''(\phi)\right) \\ &\quad\times \left[L\phi_1 - \alpha g'(\phi)\right] + O\left(\varepsilon^2\right). \end{aligned} \tag{4.55}$$

By even–odd symmetry the right-hand side of this equation is orthogonal to the translational eigenfunction ψ_1 of L. Our consistency condition, which keeps $\phi_1 = O(1)$ and determines α, requires the right-hand side be orthogonal to ψ_0,

$$\begin{aligned} &\lambda_0\left(\alpha g'(\phi) - \varepsilon A_2, \psi_0\right)_2 - \varepsilon\left(p_2'(\phi), \psi_0\right)_2 \\ &+\varepsilon\left(\left(G'''(\phi)\phi_1 + \alpha g''(\phi)\right)\left[L\phi_1 - \alpha g'(\phi)\right], \psi_0\right)_2 = 0. \end{aligned} \tag{4.56}$$

The Eq. (4.55)–(4.56) appear to be coupled, however, assuming for the moment that (4.56) has a solution, then we may solve (4.55) for ϕ_1 by projecting with $\tilde\pi$ and using the fact that $\tilde\pi L$ has an $O(1)$ inverse,

$$\phi_1 = \alpha L^{-1}\tilde\pi g'(\phi) + O(\varepsilon). \tag{4.57}$$

However, from (4.25), $\tilde\pi g'(\phi) = O(\varepsilon)$ and we see that $\phi_1 = 0$, and (4.56) reduces to

$$\begin{aligned} &\lambda_0\alpha\left(g'(\phi), \psi_0\right)_2 - \varepsilon\alpha^2\left(g''(\phi)g'(\phi), \psi_0\right)_2 \\ &\quad= \varepsilon\left(p_2'(\phi), \psi_0\right)_2 + O(\varepsilon^2). \end{aligned} \tag{4.58}$$

However using (4.25) and (4.35) we find

$$\begin{aligned} \left(g''(\phi), \left(g'(\phi)\right)^2\right)_2 &= \frac{1}{2}\int_{\mathbb{R}} g''(\phi)(\phi')^2\,\mathrm{d}z + O(\varepsilon) \\ &= \frac{1}{2}\int_{\mathbb{R}} \partial_z\left(g'(\phi)\right)\phi'\,\mathrm{d}x + O(\varepsilon), \\ &= -\frac{1}{2}\int_{\mathbb{R}} g'(\phi)\phi''\,\mathrm{d}z + O(\varepsilon) \\ &= \frac{1}{\sqrt{2}}\int_0^\infty \phi'\phi''\,\mathrm{d}z + O(\varepsilon) = O(\varepsilon), \end{aligned} \tag{4.59}$$

and using (4.22) and (4.25) to eliminate λ_0 and ψ_0 we find

$$\alpha^2 = \frac{\|\phi'\|_2\left(p_2'(\phi), \psi_0\right)_2}{2\sqrt{2\mu_+}g(b_+)} + O(\varepsilon). \tag{4.60}$$

On the other hand, using (4.25) and (4.26) again we see

$$\begin{aligned} \left(p_2'(\phi), \psi_0\right)_2 &= \frac{(p_2'(\phi), |\phi'|)_2}{\|\phi'\|_2} + O(\sqrt{\varepsilon}) \\ &= -\frac{2}{\|\phi'\|_2}\int_0^\infty p_2'(\phi)\phi'\,\mathrm{d}z \\ &= \frac{2p_2(\phi_m)}{\|\phi'\|_2} + O(\sqrt{\varepsilon}), \end{aligned} \tag{4.61}$$

so that

$$\alpha^2 = \frac{p_2(\phi_m)}{\sqrt{2\mu_+}g(b_+)} + O(\sqrt{\varepsilon}). \tag{4.62}$$

Finally, using the expression (4.18) then for $b_2 < 0$ we find the equilibrium relation

$$\alpha = \hat\alpha(b_2) = \sqrt{-\gamma_1 b_2} + O(\sqrt{\varepsilon}), \tag{4.63}$$

where

$$\gamma_1 = \sqrt{\frac{\mu_+}{2}}\frac{\mu_+(b_+ - b_-)}{g(b_+)}. \tag{4.64}$$

These results lead to the following proposition

Proposition 4.1. *For the scaling $\eta = \eta_2\varepsilon^2$ and $b = b_- + \varepsilon^2 b_2$, then the solution ϕ of (4.15) renders $\|S(\phi)\|_{L^2} = O(\varepsilon^2)$. Moreover, for the choice $\alpha(b) = \hat\alpha(b_2)$ given by (4.63) we have $(S(\Phi_0), \psi_0)_2 = O(\varepsilon^3)$. Moreover, for any admissible hypersurface $\Gamma \subset \mathbb{R}^d$*

$$\begin{aligned} &\lim_{\varepsilon\to 0^+}\varepsilon^{-3}\mathcal{F}(\phi) \\ &\quad= \|\phi'\|_2^2\int_\Gamma\left[\frac{(d-1)^2}{2}H^2 + \left(\frac{\alpha^2}{4} - \eta_2\right)\right]\mathrm{d}s. \end{aligned} \tag{4.65}$$

Proof. Recalling the energy (1.4), we must capture the leading-order non-zero contributions of each of the two terms. From (4.8) and (4.12) we see that

$$W(u) = G(u) + \varepsilon\alpha g(\phi) + O(\varepsilon^2). \tag{4.66}$$

Combining this with the change of variables (2.17) we find

$$\begin{aligned} \varepsilon^2\Delta\phi - W'(\phi) &= G'(\phi) - W'(\phi) + \varepsilon\kappa_0\phi' + O(\varepsilon^2), \\ &= \varepsilon\left(\kappa_0\phi' + \alpha g'(\phi)\right) + O(\varepsilon^2), \\ &= \varepsilon\left(\kappa_0\phi' + \alpha\|g'(\phi)\|_2\psi_0\right) + O(\varepsilon^2). \end{aligned} \tag{4.67}$$

On the other hand, from the first integral (4.29) of (4.15) we have

$$\frac{\varepsilon^2}{2}|\nabla\phi|^2 + W(\phi) = |\phi'|^2 + O(\varepsilon). \tag{4.68}$$

Inserting these identities into (1.4) and changing to whiskered coordinates yields

$$\begin{aligned} \mathcal{F}(\Phi_0) &= \varepsilon^3\int_\Gamma\int_{\mathbb{R}}\frac{1}{2}\left(\kappa_0\phi' + \frac{\alpha}{\sqrt{2}}\|\phi'\|_2\psi_0\right)^2 - \eta_2|\phi'|^2\,\mathrm{d}z\,\mathrm{d}s \\ &\quad + O(\varepsilon^4). \end{aligned} \tag{4.69}$$

The contributions to the energy from points away from the hypersurface Γ are $O(\varepsilon^4)$ and may be neglected. Performing the integration over $\mathbb{R}$, using the orthogonality of ϕ' and ψ_0 and the definition of κ_0 from (2.16), we obtain (4.65). □

From Eq. (4.65) we infer that for small values of α_1 (wide bi-layers) the energy is decreased by increasing the surface area of the hypersurface Γ, while for $\alpha_1 > 2\sqrt{\eta_2}$, the interfacial energy increases with both increasing curvature and increasing surface area. The corresponding gradient flow (1.5), with its conservation of mass, will couple the evolution of the hypersurface to the bi-layer width and the background value, as is demonstrated in the sequel.

4.3. Fully dressed bi-layer Ansatz

Recovering the leading order dynamics of a bi-layer interface under Eq. (4.14) requires a higher order Ansatz with the residual resolved to $O(\varepsilon^3)$. The bi-layer, ϕ, generated from the reduced second-order Eq. (4.15) incorporates the detuning parameter, α, and the far-field effect of the background state b. An ansatz of sufficient fidelity to resolve the leading-order normal velocity requires the incorporation of curvature dependent effects in the near-field shape of the bi-layer profile. We take the detuning parameter $\alpha = \alpha(s,t)$ and the background state $b = b(t)$ to be independent, and derive their quasi-equilibrium dependence as well as the temporal relaxation of a variable width interface, $\alpha = \alpha(s,t)$, onto a spatially uniform width interface.

The fully dressed bi-layer Ansatz takes the form,

$$\Phi(s,z;\alpha(s,t),b(t)) = \phi(z;\alpha,b) + \varepsilon^2\phi_2(s,z), \tag{4.70}$$

where $\alpha(s,t)$ is the relaxation parameter within the potential G and $b(t) = b_- + \varepsilon^2 b_2(t)$ is the background state. Due to the form of the tilt function, g, we take $\phi_1 = 0$, while ϕ_2 is a localized function to be determined. From (4.14) we see that the Ansatz has a residual

$$S(\Phi) = \left(\varepsilon^2\Delta - G''(\Phi) - \varepsilon\alpha g''(\Phi)\right)\left(\varepsilon^2\Delta\Phi - G'(\Phi) - \varepsilon\alpha g'(\Phi)\right) + p'(\Phi). \tag{4.71}$$

Recalling the whiskered form of the Laplacian, (2.17), the expansion of the extended curvature, (2.15) and (2.16), the scalings $\eta = \varepsilon^2\eta_2$, $b = b_- + \varepsilon^2 b_2$, and the asymptotic reduction $p(\Phi) = \varepsilon^2 p_2(\Phi)$ with p_2 given by (4.11), we formally expand both the prefactor and the Cahn–Hilliard residual,

$$S(\Phi) = \left(P_0 + \varepsilon P_1 + \varepsilon^2 P_2\right)\left(\varepsilon A_1 + \varepsilon^2 A_2 + \varepsilon^3 A_3\right) + \varepsilon^2 p_2'(\phi) + O(\varepsilon^4). \tag{4.72}$$

The prefactors are given by $P_0 = L$, from (4.19), and

$$P_1 = \kappa_0\partial_z - \alpha g''(\phi), \tag{4.73}$$

$$P_2 = z\kappa_1\partial_z + \Delta_s - G'''(\phi)\phi_2, \tag{4.74}$$

which operate on the Cahn–Hilliard residuals

$$A_1 = \kappa_0\phi' - \alpha g'(\phi), \tag{4.75}$$

$$A_2 = L\phi_2 + z\kappa_1\phi' + \Delta_s\phi. \tag{4.76}$$

We will see that the form of A_3 is not relevant to the dynamics. The operator L acts on near-field functions supported on the whisker neighborhood, $\Gamma(1)$, where it depends upon α and b through ϕ. On each fixed whisker, the projection $\tilde\pi$ removes the small eigenspaces of L, giving $\tilde\pi L$ an $O(1)$ inverse on that whisker.

We choose the perturbations ϕ_1 and ϕ_2 to reduce the size of the projected residual, $\tilde\pi P(\Phi)$, on each whisker. Expanding the residual in orders of ε yields

$$S(\Phi) = \varepsilon\overbrace{LA_1}^{R_1} + \varepsilon^2\overbrace{\left(LA_2 + P_1A_1 + p_2'(\phi)\right)}^{R_2} + \varepsilon^3\overbrace{\left(LA_3 + P_1A_2 + P_2A_1\right)}^{R_3} + O(\varepsilon^4). \tag{4.77}$$

The $O(\varepsilon)$ terms are all localized near the front. Using $L\phi' = 0$ and recalling (4.31), they take the form

$$R_1 \equiv -\alpha Lg'(\phi) = -\alpha\left(2\varepsilon\alpha g'''(\phi)g(\phi) + \varepsilon^2 r(\phi)\right). \tag{4.78}$$

We already have $\tilde\pi R_1 = 0$ to leading order, which is consistent with $\phi_1 = 0$, and we incorporate the higher order terms into R_2 and R_3. At $O(\varepsilon^2)$ we have

$$\tilde R_2 \equiv R_2 - 2\alpha^2 g'''(\phi)g(\phi) = LA_2 + P_1A_1 + p_2'(\phi) - 2\alpha^2 g'''(\phi)g(\phi), \tag{4.79}$$

and we render $\tilde\pi\tilde R_2 = 0$ along each whisker through the choice

$$\phi_2 = -L^{-2}\tilde\pi\left(L\tilde A_2 + P_1A_1 + p_2'(\phi) - 2\alpha^2 g'''(\phi)g(\phi)\right), \tag{4.80}$$

where $\tilde A_2 \equiv A_2 - L^2\phi_2$ is the second order Cahn–Hilliard residual obtained when $\phi_2 = 0$. In particular A_2 reduces to

$$A_2 = \pi\tilde A_2 - L^{-1}\tilde\pi\left(P_1A_1 + p_2'(\phi) - 2\alpha^2 g'''(\phi)g(\phi)\right). \tag{4.81}$$

We have constructed an Ansatz $\Phi = \Phi(x;\alpha,b)$, for which $\tilde\pi S(\Phi) = O(\varepsilon^3)$ uniformly along each whisker. Indeed,

$$S(\Phi) = \varepsilon^2\left(\tilde R_{20}\psi_0 + \tilde R_{21}\psi_1\right) + \varepsilon^3\tilde R_3 + O(\varepsilon^4) \tag{4.82}$$

where $\tilde R_{2j} \equiv (\tilde R_2, \psi_j)_2$, and

$$\tilde R_3 \equiv LA_3 + P_1A_2 + P_2A_1 - \alpha r(\phi). \tag{4.83}$$

5. Evolution of bi-layer interfaces

We resolve the time evolution of the parameters $z = z(t)$ (as a function of the hypersurface $\Gamma = \Gamma(t)$), the tilt $\alpha = \alpha(s,t)$, and the background state $b = b(t)$, for solutions of (1.5) arising from initial data u_0 from a neighborhood of the dressed manifold

$$\mathcal{M} \equiv \{\Phi(z;\alpha,b)|\Gamma \text{ admissible},\ b = b_- + \varepsilon^2 b_2, \alpha(s) > \alpha_*(b)\}. \tag{5.1}$$

For such initial data we decompose the solutions u as,

$$u(x,t) = \Phi(s,z,t) + v(x,t), \tag{5.2}$$

where Φ is the Ansatz (4.70), which depends upon time through the parameters, and v is the perturbation to the Ansatz. From the chain rule we have

$$\partial_t\Phi = z_t\phi' + \alpha_t\partial_\alpha\phi + \varepsilon^2 b_{2,t}\partial_b\phi + O(\varepsilon z_t, \varepsilon\alpha_t, \varepsilon^3 b_{2,t}). \tag{5.3}$$

We will see below that $z_t = O(\varepsilon^3)$, while α_t and $b_{2,t}$ are both $O(\varepsilon)$, so that the error terms are $O(\varepsilon^4)$. Putting the decomposition (5.2) of u into the evolution Eq. (4.14), we obtain

$$z_t\phi' + \alpha_t\partial_\alpha\phi + \varepsilon^2 b_{2,t}\partial_b\phi + v_t = -\Pi_0 S(\Phi + v) \tag{5.4}$$

or equivalently

$$z_t\phi' + \alpha_t\partial_\alpha\phi + \varepsilon^2 b_{2,t}\partial_b\phi + v_t = -\Pi_0 S(\Phi) - \mathbb{L}v - \Pi_0\mathcal{N}(v), \tag{5.5}$$

where $\mathbb{L} = \Pi_0\mathcal{L}$ and $\mathcal{N}(v)$ represent the nonlinear terms in v. While the linear operator

$$\mathcal{L} \equiv \left(\varepsilon^2\Delta - G''(\Phi) - \varepsilon\alpha g''(\Phi)\right)^2 + p''(\Phi) - G'''(\Phi) \times \left(\varepsilon^2\Delta\Phi - G'(\Phi) - \varepsilon\alpha g'(\Phi)\right), \tag{5.6}$$

is self-adjoint, $\mathbb{L}$ is not, however $\sigma(\mathbb{L}) \subset \sigma(\Pi_0\mathcal{L}\Pi_0) \cup \{0\}$, and $\sigma(\Pi_0\mathcal{L}\Pi_0)$ interleave with $\sigma(\mathcal{L})$, so that the spectral set of $\mathcal{L}$ controls that of $\mathbb{L}$. The adjoint operator $\mathbb{L}^\dagger$ has a kernel spanned by the constant function $\Psi_0^\dagger \equiv 1$. Applying the results of [35], the spectrum of $-\mathbb{L}$ is bounded above by a constant of $O\left(\varepsilon^2\|\kappa_0\|^2_{L^\infty(\Gamma)}, \varepsilon^4\eta_2^2\right)$ while there exists $\nu > 0$, independent of ε, for which the adjoint eigenspace corresponding to eigenvalues greater than $-\nu\varepsilon$ takes the form (see Fig. 5.1)

$$Y_\nu(\Omega) = \text{span}\{\Psi_0^\dagger\} \cup \{\Psi_{i,j}^\dagger | i = 0,\ 1,\ \text{and } 1 \le j \le N_\varepsilon\}. \tag{5.7}$$

Here the $\Psi_{i,j}^\dagger$ have a separated variables decomposition

$$\Psi_{0,j}^\dagger = \varepsilon^{-\frac{1}{2}}\psi_0(z;\alpha)\Theta_{0,j}(s) + \Psi_{0,j}^\perp(x), \tag{5.8}$$

$$\Psi_{1,j}^\dagger = \varepsilon^{-\frac{1}{2}}\psi_1(z;\alpha)\Theta_{1,j}(s) + \Psi_{1,j}^\perp(x), \tag{5.9}$$

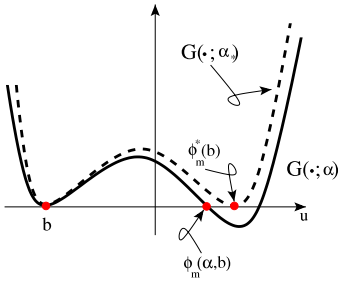

Fig. 4.1. The modified potential G for $\alpha > \alpha_*$ (solid) and $\alpha = \alpha_*$ (dotted). At $\alpha = \alpha_*$ the potential G has a double zero at $u = \phi_m^*(b)$. Increasing the value of α above α_* lowers G about its pivot point at $u = b$, where it maintains a double zero. The double zero at $u = \phi_m^*$ breaks into two zeros of G, the smaller of which, denoted ϕ_m, is also the maximum of the homoclinic pulse, ϕ.

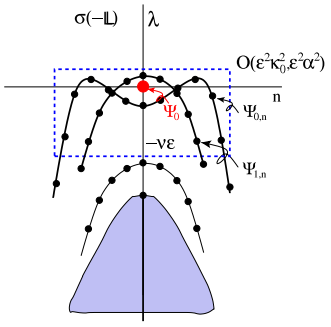

Fig. 5.1. A cartoon representation of spectrum of the operator, $-\mathbb{L}$, the negative of the linearization of the ZMFCH equation about a bi-layer dressed interface. The eigenvalues (all real) are plotted against the transverse index n, arrows connect the eigenfunctions Ψ_0, $\Psi_{0,n}$ and $\Psi_{1,n}$ to their associated eigenvalue. The bilayer mean-curvature, κ_0, and width-parameter, α, manifests their influence on the small eigenvalues through shifts of the order $O(\varepsilon^2\|\kappa_0\|^2_{L^\infty(\Gamma)}, \varepsilon^2\|\alpha\|^2_{L^\infty(\Gamma)})$.

where the corrections $\Psi^\perp_{i,j}$ are $O(\varepsilon)$ in $L^2(\Omega)$, and are orthogonal to ψ_0 and ψ_1 on each whisker. With this normalization we have $\|\Psi^\dagger_{i,j}\|_{L^2(\Omega)} = 1$. Moreover, as for the single-layer interfaces, it is shown in [35] that there exists an $N_\varepsilon > 0$ such that both of the sets

$$Y_{v,i}(\Gamma) = \{1\} \cup \left\{\Theta_{i,j} | j = 1, \ldots, N_\varepsilon\right\}, \tag{5.10}$$

for $i = 0$ and 1 form an approximate basis of $L^2(\Gamma)$ in the sense that any function f which is orthogonal to one of $Y_{v,i}(\Gamma)$ in $L^2(\Gamma)$ satisfies

$$\|f\|_{L^2(\Gamma)} \le \varepsilon c \|\Delta_s f\|_{L^2(\Gamma)}, \tag{5.11}$$

for a constant $c > 0$ which depends only upon v and Γ. The decomposition (5.2) is under-constrained, as the remainder v and the parameters α, b, are not uniquely determined by u and Γ. To eliminate this degeneracy, and eliminate secular growth of the perturbation v, we impose the non-degeneracy conditions $v \perp_{L^2(\Omega)} Y_v$. These conditions make the semigroup generated by $\mathbb{L}$ uniformly contractive on v. Defining π_v to be the $\mathcal{L}$ spectral projection onto $Y_v(\Omega)$, and $\tilde{\pi}_v = I - \pi_v$, we will show elsewhere that v remains of the same magnitude as $\tilde{\pi}_v S(\Phi)$, which from (4.82) is $O(\varepsilon^3)$, so long as Γ remains admissible under the flow. The nonlinear terms $\mathcal{N}(v)$ are yet of a higher order and may be neglected in the derivation of the leading-order shape and parameter evolution. In the sequel we derive these evolution equations by taking the $L^2(\Omega)$ projection of (5.5) against each family of adjoint eigenfunctions, exploiting the approximate basis property of $Y_{v,i}(\Gamma)$ for $i = 0, 1$. For each projection we break the integrands into near- and far-field terms, change the near-field integrals to the whiskered variables, observe the orthogonality of the terms that are linear in v, and drop the nonlinear terms in v (see Fig. 4.1).

5.1. Relaxation to a uniform bi-layer

Projecting (5.5) onto the kernel, $\Psi_0^\dagger$ of $\mathbb{L}^\dagger$, we obtain the expression for conservation of mass within the system

$$\int_\Gamma \int_{\mathbb{R}} \left[z_t \phi' + \alpha_t \partial_\alpha \phi\right] J(s,z)\, \mathrm{d}z\, \mathrm{d}s + \varepsilon^2 b_{2,t} \int_\Omega \partial_b \phi\, \mathrm{d}x = 0. \tag{5.12}$$

From the decomposition (4.43) of $\partial_b \phi$ and the Jacobian expansion (2.14) we have

$$\begin{aligned}\int_\Omega \partial_b \phi\, \mathrm{d}x &= |\Omega| - \varepsilon^{-1} \int_\Gamma \int_{\mathbb{R}} \rho_b \psi_0 J(s,z)\, \mathrm{d}s\, \mathrm{d}z + O(\varepsilon) \\ &= |\Omega| - \int_\Gamma \rho_b \overline{\psi_0}\, \mathrm{d}s + O(\varepsilon).\end{aligned} \tag{5.13}$$

From the expansion (4.40) we have

$$\int_{\mathbb{R}} \partial_\alpha \phi J(s,z)\, \mathrm{d}z = -\varepsilon \rho_\alpha \overline{\psi_0} + O(\varepsilon^2). \tag{5.14}$$

The first term on the left-hand side of (5.12) expresses the influence of the normal velocity on the hypersurface area $|\Gamma|$. The scaled normal velocity $z_t = z_t(s,t)$ is a function of position s along the hypersurface, and not distance z to the hypersurface, so the integral over the whiskers becomes

$$\begin{aligned}\int_{\mathbb{R}} \phi' J(s,z)\, \mathrm{d}z &= \varepsilon^2 \kappa_0 \int_{\mathbb{R}} \partial_z(\phi - b) z\, \mathrm{d}z + O(\varepsilon^4) \\ &= -\varepsilon^2 \kappa_0 M_b + O(\varepsilon^4),\end{aligned} \tag{5.15}$$

where

$$M_b(\alpha, b) \equiv \int_{\mathbb{R}} (\phi - b)\, \mathrm{d}z, \tag{5.16}$$

denotes the mass of the homoclinic above the background state. The full integral of this term expresses the rate of change of mass in the bi-layer arising from stretching by the geometric flow,

$$\int_\Gamma \int_{\mathbb{R}} z_t \phi' J(s,z)\, \mathrm{d}z\, \mathrm{d}s = -\varepsilon^2 \int_\Gamma z_t \kappa_0 M_b\, \mathrm{d}s. \tag{5.17}$$

Factoring out an ε term, the mass conservation Eq. (5.12) takes the form

$$\int_\Gamma \Big[\overbrace{\left(\rho_\alpha \alpha_t + \varepsilon \rho_b b_{2,t}\right)\overline{\psi_0}}^{\text{widening}} + \overbrace{\varepsilon z_t \kappa_0 M_b}^{\text{stretching}}\Big]\, \mathrm{d}s = \overbrace{\varepsilon |\Omega| b_{2,t}}^{\text{background}}, \tag{5.18}$$

to a leading order in each term. The distribution of mass within the system can change by stretching the hypersurface, local changes of the width of the bi-layer, or varying the background state.

To address the evolution of the detuning parameter α we project (5.5) onto $\Psi^\dagger_{0,j}$. As all terms are localized on the front we may change the integral to the whiskered coordinates,

$$\begin{aligned}&\int_\Gamma \int_{\mathbb{R}} \left(z_t \phi' + \alpha_t \partial_\alpha \phi + \varepsilon^2 b_{2,t} \partial_b \phi\right) \Psi^\dagger_{0,j} J(s,z)\, \mathrm{d}z\, \mathrm{d}s \\ &= -\int_\Gamma \int_{\mathbb{R}} \Psi^\dagger_{0,j} \Pi_0 S(\Phi) J(s,z)\, \mathrm{d}z\, \mathrm{d}s.\end{aligned} \tag{5.19}$$

Expanding the Jacobian and $\Psi^\dagger_{0,j}$ according to (2.14) and (5.8) respectively, neglecting the lower order $\Psi^\perp_{0,j}$ corrections, and dividing the equation by ε, the leading order terms are

$$\begin{aligned}&\int_\Gamma \left(\varepsilon z_t (z\phi', \psi_0)_2 \kappa_0 - \alpha_t \rho_\alpha - \varepsilon b_{2,t} \rho_b\right) \Theta_{0,j}(s)\, \mathrm{d}s \\ &= -\int_\Gamma \Theta_{0,j}(s) (\Pi_0 S(\Phi), \psi_0)_2\, \mathrm{d}s.\end{aligned} \tag{5.20}$$

The set $Y_{v,0}(\Gamma)$ forms an approximate basis, so assuming the admissibility Γ, and hence smoothness of the curvatures, as well as smoothness of α is s, the integrands must agree to leading order, yielding

$$\alpha_t \rho_\alpha + \varepsilon z_t \kappa_0 \rho_z(\alpha) + \varepsilon b_{2,t} \rho_b = (\Pi_0 S(\Phi), \psi_0)_2, \tag{5.21}$$

where we have introduced

$$\rho_z(\alpha) \equiv -(z\phi', \psi_0)_2 = -\frac{(z, \partial_z g(\phi))_2}{\|g'(\phi)\|_2} + O(\varepsilon) = \frac{\overline{g(\phi)}}{\|g'(\phi)\|_2} + O(\varepsilon) > 0. \tag{5.22}$$

Turning to the right-hand side of (5.21) we see from (4.82) that $S(\Phi)$ is localized and its mass over all of Ω is of a higher order, so that

$$\Pi_0 S(\Phi) = \varepsilon^2 \left(\tilde{R}_{20}\psi_0 + \tilde{R}_{21}\psi_1\right) + O(\varepsilon^3). \tag{5.23}$$

The solvability condition (4.63) is precisely the vanishing of $\tilde{R}_{20}$, which we now derive through the dynamics. Integrating against ψ_0 on each whisker we obtain

$$(\Pi_0 S(\Phi), \psi_0)_2 = \varepsilon^2 \tilde{R}_{20} + O(\varepsilon^3), \tag{5.24}$$

where from (4.79) we have

$$\tilde{R}_{20} = \left(LA_2 + P_1 A_1 + p_2'(\phi) - 2\alpha^2 g'''(\phi) g(\phi), \psi_0\right)_2, \tag{5.25}$$

however the LA_2 term can be neglected as $L\psi_0 = \lambda_0\psi_0 = O(\varepsilon)$ renders it a lower order. Expanding the second term, and exploiting even–odd cancellations yields

$$(P_1 A_1, \psi_0)_2 = \kappa_0^2 \left(\phi'', \psi_0\right)_2 + \alpha^2 \left(g''(\phi) g'(\phi), \psi_0\right)_2. \tag{5.26}$$

We see from (A.6) that $\left(\phi'', \psi_0\right)_2 = \frac{1}{2}\left(L(z\phi'), \psi_0\right) = \frac{1}{2}\lambda_0 \rho_z(\alpha)$, which is $O(\varepsilon)$. Similarly from (4.58) and the line below it, the second inner product on the right-hand side of (5.26) is also $O(\varepsilon)$. To address the remaining terms in (5.25) we recall the derivation of (4.63) which leads us to the expression

$$(\Pi_0 S(\Phi), \psi_0)_2 = -\frac{2\sqrt{2}\,\gamma_0}{\|\phi'\|_2}\left(\alpha^2 - \hat{\alpha}^2(b)\right) + O(\varepsilon). \tag{5.27}$$

In particular, the evolution Eq. (5.21) reduces to

$$\alpha_t \rho_\alpha + \varepsilon z_t \kappa_0 \rho_z(\alpha) + \varepsilon b_{2,t} \rho_b = -\frac{2\sqrt{2}\,\gamma_0 \varepsilon^2}{\|\phi'\|_2}\left(\alpha^2 - \hat{\alpha}^2(b)\right) + O(\varepsilon). \tag{5.28}$$

In the sequel it will be shown that $z_t = O(\varepsilon^3)$ and hence this term is of a lower order in both (5.18) and (5.28). These two equations describe the leading order evolution of the background state and the bi-layer width. Moreover they can be uncoupled at the leading order. We first observe from (4.23) that γ_0 is independent of α to a leading order. We can obtain the same result for $\|\phi'\|_2$ since

$$\partial_\alpha \|\phi'\|_2^2 = -2\left(\partial_\alpha \phi, \phi''\right)_2 = -\frac{1}{2}\left(L\partial_\alpha\phi, z\phi'\right)_2 + O(\varepsilon) = \varepsilon\alpha\left(g'(\phi), z\phi'\right)_2 + O(\varepsilon) = O(\varepsilon), \tag{5.29}$$

where we used (4.45) and (A.6) to obtain the second and third equalities. Introducing the surface-weighted average

$$\langle f \rangle_0 = \frac{\int_\Gamma f(s)\overline{\psi_0}(s)\,\mathrm{d}S}{\int_\Gamma \overline{\psi_0}(s)\,\mathrm{d}S}, \tag{5.30}$$

we multiply (5.28) by $\overline{\psi_0}$ and integrate over Γ and use the result to replace the "widening" terms in (5.18). Dropping the lower-order "stretching" terms, we obtain the leading order evolution equation for the background state,

$$b_{2,t} = -\frac{2\sqrt{2}\varepsilon\,\gamma_0 \int_\Gamma \overline{\psi_0}\mathrm{d}S}{\|\phi'\|_2 |\Omega|}\left\langle \alpha^2 - \hat{\alpha}^2(b_2)\right\rangle_0 + O\left(\varepsilon^2\right). \tag{5.31}$$

Returning to (5.28), and dropping the lower order stretching term we have the evolution

$$\alpha_t + \varepsilon\frac{\rho_b}{\rho_\alpha} b_{2,t} = -\frac{2\sqrt{2}\,\gamma_0 \varepsilon^2}{\|\phi'\|_2 \rho_\alpha}\left(\alpha^2 - \hat{\alpha}^2(b_2)\right) + O(\varepsilon^3). \tag{5.32}$$

The evolution for the background perturbation b_2 takes place on a relatively fast $t = O(\varepsilon^{-1})$ time-scale while the bi-layer width seeks its equilibrium on a $t = O(\varepsilon^{-2})$ time-scale. We may view α as a constant over the $t = O(\varepsilon^{-1})$ time-scale. Recalling the equilibrium relation (4.63), we see that b_2 solves a linear equation

$$b_{2,t} = -\frac{2\sqrt{2}\varepsilon\,\gamma_0 \int_\Gamma \overline{\psi_0}\mathrm{d}S}{\|\phi'\|_2 |\Omega|}\left(\left\langle\alpha^2\right\rangle_0 + \gamma_1 b_2\right) + O\left(\varepsilon^{\frac{3}{2}}\right). \tag{5.33}$$

In particular, b_2 relaxes after an $O(\varepsilon^{-1})$ transient to its stable equilibrium value

$$\hat{b}_2(\alpha) \equiv -\frac{\left\langle\alpha^2\right\rangle_0}{\gamma_1} < 0. \tag{5.34}$$

Subsequently, the background state is driven adiabatically by the relaxation parameter and its time derivative scales as $b_{2,t} = O(\|\alpha_t\|_\infty) = O(\varepsilon^2)$. On the longer $t = O(\varepsilon^{-2})$ time-scales the $b_{2,t}$ term on the left-hand side of (5.32) may be neglected, yielding a nonlinear-nonlocal system of ODEs for $\alpha(s,t)$ with a common equilibrium value given by the nonlocal term $\hat{b}_2$. Moreover the equilibrium value of b_2 is precisely the value that makes the right-hand side of (5.31) zero, viz. $\left\langle\alpha^2\right\rangle_0 = -\left\langle\hat{\alpha}^2(b_2)\right\rangle_0$. Substituting from (4.23) and (4.41) to simplify the leading coefficient, the system (5.32) takes the appealing closed form

$$\alpha_t(s,t) = -16\varepsilon^2 \frac{\mu_+ g^2(b_+)}{\|\phi'\|_2^2}\alpha\left(\alpha^2 - \left\langle\alpha^2\right\rangle_0\right) + O(\varepsilon^{\frac{5}{2}}). \tag{5.35}$$

This equation has a family of equilibria comprised of functions that are constant in the transverse variable s. To address the linear stability of this family, we consider zero mass perturbations w to a constant background state $\alpha(s) = \alpha_0 + w(s)$, where $\|w\| \ll 1$. Such perturbations do not impact the surface-weighted average operator at a linear level. Indeed taking the variational derivative, the contributions from $\partial_\alpha\overline{\psi_0}$ cancel since α_0 is constant in s, and we have

$$\frac{\delta\left\langle\alpha^2\right\rangle_0}{\delta\alpha}(w) = 2\alpha_0\left\langle w(s)\right\rangle_0 = 0. \tag{5.36}$$

Modulo perturbations to the total mass, which merely shift the constant value of α, the linearization of the nonlocal system (5.35) uncouples into ODEs with a common equilibrium value, and the linear stability of the family of uniform states follows.

The actual equilibrium values α and $\hat{b}(\alpha) \equiv b_- + \varepsilon^2\hat{b}_2(\alpha)$ attained depend upon the initial mass of u_0 and the area $|\Gamma|$ of the hypersurface. Since the remainder v in (5.2) satisfies the non-degeneracy conditions, and in particular has zero mass, we have the equality

$$\begin{aligned}\int_\Omega u_0(x)\,\mathrm{d}x &= \int_\Omega u(x,t)\,\mathrm{d}x = \int_\Omega \Phi(z,\alpha,\hat{b}(\alpha))\,\mathrm{d}x,\\ &= \int_\Omega \left(\hat{b}(\alpha) + \left(\phi(z;\alpha,\hat{b}(\alpha)) - \hat{b}(\alpha)\right) + \varepsilon^2\phi_2\right)\mathrm{d}x,\\ &= \hat{b}(\alpha)|\Omega| + \varepsilon\int_\Gamma M_b(\alpha,\hat{b}(\alpha))\,\mathrm{d}s + O(\varepsilon^3|\Gamma|),\\ &= |\Omega|b_- + \varepsilon|\Gamma|M_b(\alpha,\hat{b}(\alpha)) + O(\varepsilon^2).\end{aligned} \tag{5.37}$$

An initial datum close to $\mathcal{M}$ has a mass of the form $\int_\Omega u_0(x)\,dx = |\Omega|b_- + \varepsilon m_0$, for some $m_0 > 0$ independent of ε. The quasi-steady value of α satisfies the equality

$$M_b(\alpha) = \frac{m_0}{|\Gamma|} + O(\varepsilon). \tag{5.38}$$

From Lemma A.3 we see that M_b is strictly decreasing in α with a logarithmic singularity as $\alpha \to \alpha_*^+$. The intermediate value theorem provides the existence of a unique solution $\alpha = \alpha(m_0, |\Gamma|)$ of (5.38) for admissible curves Γ and sufficiently large (scaled) initial masses m_0.

5.2. Geometric evolution of bi-layer interfaces

We assume that the detuning and background parameters have relaxed to their quasi-equilibria, which we denote with the unadorned α and b. The evolution of the hypersurface, Γ, couples to these quasi-equilibria through (5.38) since the changes in hypersurface area, while slow, are cumulative and will compete for mass. We introduce the slow time $\tau = \varepsilon^3 t$ and the normal velocity $\mathbf{V}_\mathrm{n} = -z_\tau = -\varepsilon^{-3} z_t$. As the parameters are driven by the interface evolution, we assume that $\alpha_\tau = b_{2,\tau} = O(1)$ in this regime. To address the geometric evolution of the hypersurface, as characterized by the leading order extended curvature, κ_0, we project (5.5) onto $\Psi_{1,j}^\dagger$, for each $j = 1, \ldots, N_\varepsilon$, and change to the whiskered coordinates,

$$\begin{aligned}&\int_\Gamma \int_{\mathbb{R}} \left(-\varepsilon^3 \mathbf{V}_\mathrm{n}\phi' + \varepsilon^3 \alpha_\tau \partial_\alpha \phi + \varepsilon^5 b_{2,\tau}\partial_b \phi\right) \Psi_{1,j}^\dagger J(s,z)\,dz\,ds \\ &= -\int_\Gamma \int_{\mathbb{R}} \Psi_{1,j}^\dagger \Pi_0 S(\Phi) J(s,z)\,dz\,ds.\end{aligned} \tag{5.39}$$

Expanding the Jacobian and $\Psi_{1,j}^\dagger$ according to (2.14) and (5.9) respectively, expanding $\partial_\alpha\phi$ and $\partial_b\phi$ according to (4.40) and (4.43), and dividing by ε we obtain,

$$\begin{aligned}&\int_\Gamma \left(-\varepsilon^3 \mathbf{V}_\mathrm{n}\|\phi'\|_2 + \rho_z(\alpha)\kappa_0\left(\varepsilon^4\alpha_\tau\rho_\alpha + \varepsilon^5 b_{2,\tau}\rho_b\right)\right)\Theta_{1,j}(s)\,ds \\ &= -\int_\Gamma \Theta_{1,j}(s)\left[(\Pi_0 S(\Phi), \psi_1(1+\varepsilon z\kappa_0))_2\right] ds \\ &\quad - \varepsilon^{\frac{1}{2}} \int_\Gamma \left(\Pi_0 S(\Phi), \Psi_{1,j}^\perp\right)_2 ds + O(\varepsilon^4)\end{aligned} \tag{5.40}$$

where $\rho_z(\alpha)$, defined in (5.22), arises from the second order terms in the Jacobian expansion.

To simplify (5.40) we observe that $\Pi_0 S(\Phi) = S(\Phi) - \langle S(\Phi)\rangle_\Omega$, the residual $S(\Phi)$ is localized so that its average value $\langle S(\Phi)\rangle_\Omega$ is smaller than $S(\Phi)$ by a factor of ε. Moreover $(\langle S(\Phi)\rangle, \psi_1)_2 = 0$ and the contribution from $\langle S(\Phi)\rangle_\Omega$ is in fact a $O(\varepsilon^2)$ lower order; so we may drop Π_0 in the first integral on the right-hand side above. Moreover, from (5.23) we see that the $O(\varepsilon^2)$ terms in $S(\Phi)$ lie in $\mathcal{R}(\pi)$ on each whisker and are thus orthogonal to the correction term $\Psi_{1,j}^\perp$. The correction term projects only onto the cubic R_3 term from $S(\Phi)$, which is localized on the whiskers and hence satisfies $\|R_3\|_{L^2(\Omega)} = O\left(\varepsilon^{\frac{1}{2}}|\Gamma|^{\frac{1}{2}}\right)$. Since $\|\Psi_{1,j}^\perp\|_{L^2(\Omega)} = O(\varepsilon)$ we see that the projection of the residual onto the correction term satisfies the inequality

$$\begin{aligned}\varepsilon^{\frac{1}{2}}\left|\int_\Gamma \left(\Pi_0 S(\Phi), \Psi_{1,j}^\perp\right)_2 ds\right| &\le c\left|\varepsilon^{-\frac{1}{2}}\int_\Omega \varepsilon^3 R_3 \Psi_{1,j}^\perp\,dx\right| \\ &\le \varepsilon^{\frac{5}{2}}\|R_3\|_{L^2(\Omega)}\|\Psi_{1,j}^\perp\|_{L^2(\Omega)} \\ &\le c\varepsilon^4|\Gamma|,\end{aligned} \tag{5.41}$$

and is a lower order for $|\Gamma| \ll \varepsilon^{-1}$. The contribution from the evolution of the detuning parameter and the background are at most $O(\varepsilon^4)$ and are neglected.

Assuming uniform bounds on the curvatures of Γ in $H^1(\Gamma)$, the approximate basis property of $Y_{\nu,1}(\Gamma)$ permits us to equate the two integrands of (5.40) at the leading order,

$$\mathbf{V}_\mathrm{n} = \varepsilon^{-3}\frac{(S(\Phi),\psi_1)_2}{\|\phi'\|_2} + \varepsilon^{-2}\kappa_0\frac{(S(\Phi), z\psi_1)_2}{\|\phi'\|_2} + O(\varepsilon). \tag{5.42}$$

The quasi-equilibrium of α and b implies that $\tilde{R}_{20} = O(\varepsilon)$. Using this fact while expanding the residual from (4.82), we obtain

$$\mathbf{V}_\mathrm{n} = \frac{1}{\|\phi'\|_2}\left(\varepsilon^{-1}\tilde{R}_{21} + \tilde{R}_{31}\right) + O(\varepsilon), \tag{5.43}$$

where $\tilde{R}_{31} \equiv (\tilde{R}_3, \psi_1)_2$.

A key fact, which both complicates the analysis and enriches the dynamics of the front evolution, is that the leading order term is degenerate, bringing higher-order effects into play. From (4.79) the $O(\varepsilon^{-1})$ term in (5.43) takes the from

$$\tilde{R}_{21} = \left(LA_2 + P_1A_1 + p_2'(\phi) - 2\alpha^2 g'''(\phi)g(\phi), \psi_1\right)_2. \tag{5.44}$$

However $L\psi_1 = 0$, while using (4.73) and (4.75) to expand P_1A_1 and exploiting parity we find

$$\begin{aligned}\tilde{R}_{21} &= -\frac{2\alpha\kappa_0}{\|\phi'\|}(\partial_z g'(\phi), \phi')_2 = \frac{\alpha\kappa_0}{\|\phi'\|}\left(Lg'(\phi), z\phi'\right)_2 \\ &= -\frac{2\varepsilon\alpha^2\kappa_0}{\|\phi'\|}\left(g'''(\phi)g(\phi), z\phi'\right)_2,\end{aligned} \tag{5.45}$$

where we used (4.31) and (A.6) in the reduction above. The normal velocity takes the form

$$\mathbf{V}_\mathrm{n} = \frac{\tilde{R}_{31}}{\|\phi'\|_2} - \frac{2\alpha^2\kappa_0}{\|\phi'\|_2^2}\left(g'''(\phi)g(\phi), z\phi'\right)_2 + O(\varepsilon). \tag{5.46}$$

This analysis justifies our scaling, as $\mathbf{V}_\mathrm{n} = O(1)$, particularly since (5.46) was obtained for an arbitrary detuning profile $\alpha(s)$ and is independent of the relaxation of α to a uniform value over the interface.

To obtain an explicit representation for the normal velocity we must expand $\tilde{R}_{31}$. Turning to (4.83) we observe that $(LA_3, \psi_1)_2 = (A_3, L\psi_1)_2 = 0$, while from (4.32) and parity considerations we find that $(r(\phi), \psi_1)_2 = 0$. We are left with

$$\tilde{R}_{31} = (P_1A_2 + P_2A_1, \psi_1)_2. \tag{5.47}$$

We address the P_1A_2 term first. Since the equilibrium value of α is constant in the tangential coordinate s, we may drop $\Delta_s\phi$ in (4.76) and expand the inner product as

$$\begin{aligned}(P_1A_2, \psi_1)_2 &= \left(L\phi_2 + \kappa_1 z\phi', P_1^\dagger\psi_1\right)_2 = \left(L^2\phi_2, L^{-1}\tilde{\pi}P_1^\dagger\psi_1\right)_2 \\ &\quad + \frac{\kappa_0\kappa_1}{2}\|\phi'\|_2.\end{aligned} \tag{5.48}$$

From (4.25), (A.6) and (A.7) we calculate

$$L^{-1}\tilde{\pi}P_1^\dagger\psi_1 = -\tilde{\pi}\left(\frac{\kappa_0}{2}z\psi_1 + \frac{\alpha}{2\sqrt{2}}z\psi_0\right) + O(\varepsilon), \tag{5.49}$$

so that (5.48) reduces to

$$\begin{aligned}(P_1A_2, \psi_1)_2 &= -\frac{\kappa_0}{2\|\phi'\|_2}\left(L^2\phi_2, z\phi'\right)_2 - \frac{\alpha}{2\sqrt{2}}\left(L^2\phi_2, z\psi_0\right)_2 \\ &\quad + \frac{\kappa_0\kappa_1}{2}\|\phi'\|_2.\end{aligned} \tag{5.50}$$

Using (4.74), (4.75) and (4.25) we expand P_2A_1 as

$$\begin{aligned}P_2A_1 &= \kappa_0\kappa_1 z\phi'' - \alpha\kappa_1 g''(\phi)z\phi' + \phi'\Delta_s\kappa_0 - \kappa_0 G'''(\phi)\phi_2\phi' \\ &\quad + \alpha\frac{\|\phi'\|_2}{\sqrt{2}}G'''(\phi)\phi_2\psi_0 + O(\varepsilon).\end{aligned} \tag{5.51}$$

Projecting onto ψ_1 we obtain

$$(P_2A_1,\psi_1)_2 = \|\phi'\|_2\left(\Delta_s\kappa_0 - \frac{\kappa_0\kappa_1}{2}\right) - \frac{\kappa_0}{\|\phi'\|_2}\left(G'''(\phi)(\phi')^2,\phi_2\right)_2 + \frac{\alpha}{\sqrt{2}}\left(G'''(\phi)\phi'\psi_0,\phi_2\right)_2. \tag{5.52}$$

We use (A.4) and (A.6) on the second inner product to write $G'''(\phi)(\phi')^2 = \frac{1}{2}L^2(z\phi')$, while (A.5) and (A.7) applied to the third term shows that $G'''(\phi)\phi'\psi_0 = \frac{1}{2}L^2(z\psi_0) + O(\varepsilon)$. Using these identities in (5.52) and using that result and (5.50) in (5.47) we obtain

$$\tilde{R}_{31} = \|\phi'\|_2\Delta_s\kappa_0 - \frac{\kappa_0}{\|\phi'\|_2}\left(L^2\phi_2, z\phi'\right)_2 + O(\varepsilon). \tag{5.53}$$

Returning to the definition, (4.80), of ϕ_2, we expand P_1A_1 and neglect terms that are odd about $z=0$ to obtain

$$L^2\phi_2 = -\tilde{\pi}\left(\kappa_1 Lz\phi' + \kappa_0^2\phi'' + \alpha^2\left[g'(\phi)g''(\phi) - 2g'''(\phi)g(\phi)\right] + p_2'(\phi)\right). \tag{5.54}$$

It is straightforward to compute that

$$\tilde{\pi}z\phi' = z\phi' + \rho_z(\alpha)\psi_0, \tag{5.55}$$

and hence $\left(Lz\phi',\tilde{\pi}z\phi'\right)_2 = -\|\phi'\|_2^2 + O(\varepsilon)$ and $\left(\tilde{\pi}\phi'',z\phi'\right)_2 = -\frac{1}{2}\|\phi'\|_2 + O(\varepsilon)$. Combining this with (4.61) we have

$$\left(p_2'(\phi),\tilde{\pi}z\phi'\right)_2 = \left(\partial_z p_2(\phi),z\right)_2 + \rho_z(\alpha)\left(p_2'(\phi),\psi_0\right)_2 = -\overline{p_2(\phi)} + \frac{2\rho_z(\alpha)p_2(\phi_m)}{\|\phi'\|_2} + O(\sqrt{\varepsilon}). \tag{5.56}$$

Combining these relations with (5.53), we obtain

$$\frac{\tilde{R}_{31}}{\|\phi'\|_2} = \left(\Delta_s - \kappa_1 - \frac{1}{2}\kappa_0^2\right)\kappa_0 - \frac{\kappa_0}{\|\phi'\|_2^2}\left(\overline{p_2(\phi)} - \frac{2\rho_z p_2(\phi_m)}{\|\phi'\|_2} + \alpha^2\left(2g'''(\phi)g(\phi) - g''(\phi)g'(\phi),\tilde{\pi}z\phi'\right)_2\right). \tag{5.57}$$

We expand $\tilde{\pi}z\phi'$ according to (5.55) and from (4.25) and (4.35) we find that the term $\left(g'(\phi)g''(\phi),\psi_0\right)_2 = O(\varepsilon)$ is a lower order, and moreover

$$\left(g''(\phi)g'(\phi),z\phi'\right)_2 = \frac{1}{2}\left(\partial_z(g'(\phi))^2,z\right)_2 = -\frac{1}{4}\|\phi'\|_2^2. \tag{5.58}$$

From (4.23) we have the expansion

$$(g'''(\phi)g(\phi),\psi_0)_2 = -\frac{\sqrt{2}\gamma_0}{\|\phi'\|_2} + O(\varepsilon), \tag{5.59}$$

while observing that $g(s)g'''(s) = \partial_s\left(g(s)g''(s) - \frac{1}{2}(g'(s))^2\right)$ we write

$$\begin{aligned}
&\int_{\mathbb{R}} g(\phi)g'''(\phi)z\phi'\,\mathrm{d}z \\
&= \int_{\mathbb{R}} z\,\partial_z\left(g(\phi)g''(\phi) - \frac{1}{2}(g'(\phi))^2\right)\mathrm{d}z, && (5.60)\\
&= -\int_{\mathbb{R}} g(\phi)g''(\phi) - \frac{1}{2}(g'(\phi))^2\,\mathrm{d}z, && (5.61)\\
&= \frac{1}{4}\|\phi'\|_2^2 - \int_{\mathbb{R}} g(\phi)\phi''\,\mathrm{d}z + O(\varepsilon), && (5.62)\\
&= \frac{1}{4}\|\phi'\|_2^2 + \int_{\mathbb{R}} g'(\phi)(\phi')^2\,\mathrm{d}z + O(\varepsilon)\\
&= \frac{1}{4}\|\phi'\|_2^2 + \frac{1}{\sqrt{2}}\|\phi'\|_3^3 + O(\varepsilon), && (5.63)
\end{aligned}$$

where we used $g''(\phi) = G'(\phi) + O(\varepsilon) = \phi'' + O(\varepsilon)$ to arrive at (5.62). Inserting these reductions into (5.46) and (5.57) yields the form of the normal velocity

$$\mathbf{V}_{\mathrm{n}} = \left(\Delta_s - \beta(\alpha) - \kappa_1 - \frac{1}{2}\kappa_0^2\right)\kappa_0 + O(\varepsilon), \tag{5.64}$$

where the α dependent coefficient β is defined by

$$\beta(\alpha) = \frac{1}{\|\phi'\|_2^2}\left(\overline{p_2(\phi)} - \frac{\rho_z(\alpha)p_2(\phi_m)}{\|\phi'\|_2} + \alpha^2\left(\frac{5\|\phi'\|_2^2}{4} + \frac{4\|\phi'\|_3^3}{\sqrt{2}} - \frac{2\sqrt{2}\gamma_0\rho_z(\alpha)}{\|\phi'\|_2}\right)\right). \tag{5.65}$$

We deduce properties of β in the lemma below.

Lemma 5.1. *The coefficient β has the asymptotic form*

$$\beta(\alpha) = -\eta_2 + \alpha^2\left(\frac{5}{4} + \frac{\mu_-^2}{\gamma_1\|\phi'\|_2^2}M_b(\alpha) + \frac{4\|\phi'\|_3^3}{\sqrt{2}\|\phi'\|_2^2} - \frac{3\sqrt{2}\gamma_0}{\|\phi'\|_2^3}\rho_z(\alpha)\right) + O(\varepsilon). \tag{5.66}$$

In particular

$$\lim_{\alpha\to\alpha_*^+}\beta(\alpha) = -\eta_2 + O(\varepsilon) < 0, \tag{5.67}$$

while there exists $\alpha_c > 0$ such that $\beta(\alpha) > 0$ for $\alpha > \alpha_c$, and β has at least one zero for $\alpha \in (\alpha_*,\alpha_c)$.

Proof. Write $\beta = (\beta_p + \alpha^2\beta_g)\|\phi'\|_2^{-2}$ where β_p represents the first two terms on the right-hand side of (5.65) which involve p_2 and β_g represents the inner products which involve g. From (4.11) we see that

$$\overline{p_2(\phi)} = \overline{p_{20}(\phi)}b_2 + \overline{p_{21}(\phi)}\eta_2 + O(\varepsilon). \tag{5.68}$$

Since $W = G + O(\varepsilon)$, we may use the relations $W'(\phi) = \phi'' + O(\varepsilon)$ and $W(\phi) = \frac{1}{2}(\phi')^2 + O(\varepsilon)$, to eliminate $W(\phi)$ and $W'(\phi)$, obtaining

$$\overline{p_{20}(\phi)} = \mu_-\int_{\mathbb{R}}\phi'' - \mu_-(\phi - b)\,\mathrm{d}z + O(\varepsilon) = -\mu_-^2M_b(\alpha) + O(\varepsilon). \tag{5.69}$$

Similarly we find

$$\overline{p_{21}(\phi)} = \int_{\mathbb{R}}\frac{1}{2}\phi''(\phi - b) - \frac{1}{2}|\phi'|^2\,\mathrm{d}z + O(\varepsilon) = -\|\phi'\|_2^2 + O(\varepsilon). \tag{5.70}$$

Combining these results with the equilibrium value of b_2 given in (5.34) yields

$$\overline{p_2(\phi)} = \frac{\mu_-^2}{\gamma_1}M_b(\alpha)\alpha^2 - \|\phi'\|_2^2\eta_2 + O(\sqrt{\varepsilon}). \tag{5.71}$$

From (4.18) and (5.34) the equilibrium value of $p_2(\phi_m)$ takes the form

$$p_2(\phi_m) = \sqrt{2\mu_+}g(b_+)\alpha^2 + O(\sqrt{\varepsilon}). \tag{5.72}$$

We combine (5.71) and (5.72) to obtain

$$\beta_p = \alpha^2\left(\frac{\mu_-^2}{\gamma_1}M_b(\alpha) - \frac{\rho_z(\alpha)\sqrt{2\mu_+}g(b_+)}{\|\phi'\|_2}\right) - \|\phi'\|_2^2\eta_2 + O(\sqrt{\varepsilon}). \tag{5.73}$$

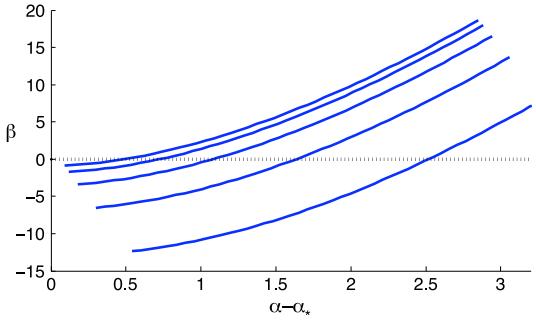

Fig. 5.2. (Left) The parameter β verses α calculated from (5.65) for a double well potential $W(s) = (1-s^2)^2/4$, $\varepsilon = 0.02$, b_2 given by the equilibrium relation (4.63), and values of $\eta_2 = 1, 2, 4, 8, 16$ which yield the curves from highest to lowest.

Combining this expression with (5.65) we obtain (5.66). Using the results of Lemmas A.3 and A.4, we see that M_b and ρ_z have logarithmic singularities as $\alpha \to \alpha_*^+ = O(\varepsilon)$, however these are dominated by the α^2 prefactor, and we obtain (5.67). From Lemma A.4 we see that both M_b and ρ_z are positive but decrease with increasing α. In particular, for α sufficiently large, independent of ε, we have the lower bound $\beta(\alpha) \geq -\eta_2 + c\alpha^2$, for a $c > 0$ also independent of ε. Taking $\alpha_c > \sqrt{\eta_2/c}$ shows that $\beta > 0$ for $\alpha > \alpha_c$. (see Fig. 5.2) □

5.3. Coupled evolution

The normal velocity couples to the tilt parameter α through the parameter β in (5.64). The evolution of the curve shape couples back to α through (5.38). The interfacial surface area $|\Gamma|$ evolves according to a curvature weighted integral of the normal velocity,

$$|\dot{\Gamma}| = \int_\Gamma V_n \kappa_0 \, \mathrm{d}s. \tag{5.74}$$

Substituting (5.64) and integrating the Laplace–Beltrami operator by parts over the closed curve Γ we obtain

$$|\dot{\Gamma}| = \int_\Gamma -|\nabla_s \kappa_0|^2 - \left(\beta + \kappa_1 + \frac{1}{2}\kappa_0^2\right)\kappa_0^2 \, \mathrm{d}s. \tag{5.75}$$

The relation between κ_0 and κ_1 is in general complicated. However for a single, radially symmetric interface, then each curvature $k_i = 1/R$ where R is the radius of Γ, so that $\kappa_0 = \frac{d-1}{R}$, $\kappa_1 = -\frac{d-1}{R^2}$, and moreover $\dot{R} = V_n$. For this case we have the simple expression

$$|\dot{\Gamma}| = -S_d \left(\beta + \frac{(d-1)(d-3)}{2R^2}\right)(d-1)^2 R^{d-3}, \tag{5.76}$$

where S_d is the surface area of the unit ball in $\mathbb{R}^d$. The radius evolves according to the coupled system

$$\dot{R} = -\left(\beta(\alpha) + \frac{(d-1)(d-3)}{2R^2}\right)\frac{d-1}{R}, \tag{5.77}$$

$$M_b(\alpha) = \frac{m_0}{S_d R^{d-1}}. \tag{5.78}$$

For $d \neq 3$ the unique equilibrium is determined by solving

$$R = \sqrt{\frac{(d-1)(d-3)}{2\beta(\alpha)}}, \tag{5.79}$$

coupled to (5.78). In particular the equilibrium occurs for an α with $\beta(\alpha) > 0$ for $d = 2$ and with $\beta(\alpha) < 0$ for $d \geq 4$. In $\mathbb{R}^3$, the equilibrium occurs for $\beta(\alpha) = 0$ with associated radius $R = (m_0/M_b(\alpha)/S_3)^{\frac{1}{3}}$, so that the equilibrium value of the detuning parameter, and consequently the bi-layer width is independent of the initial mass parameter, m_0.

5.4. Two-dimensional results

As for the front-type interfaces, the normal velocity may be rewritten in terms of the curvature, which in $\mathbb{R}^2$ takes the form

$$\partial_\tau \kappa_0 + \left(\int_0^s \mathbf{V}_n \kappa_0(s)\, \mathrm{d}s\right)\partial_s \kappa_0 = -\left(\partial_s^2 + \kappa_0^2\right)\left(\partial_s^2 - \beta + \frac{1}{2}\kappa_0^2\right)\kappa_0 + O(\varepsilon). \tag{5.80}$$

5.4.1. Stability of radially symmetric solutions

To address the stability of this stationary solution with respect to non-radial perturbations, we consider a surface $\Gamma \subset \mathbb{R}^2$ whose curvature is a small perturbation from a constant value, $\kappa_0 = \overline{\kappa}_0 + v(s,\tau)$, where $\overline{\kappa}$ solves $V_n(\overline{\kappa}) = 0$ and $\|v\|_{L^\infty(\Gamma)} \ll 1$. To determine the linearized equation we must address the variation of the equilibrium relation $\alpha = \alpha(|\Gamma|)$, given by (5.38), with respect to κ_0. By the chain rule we have may define the variational derivative of β with respect to perturbations to κ_0,

$$\frac{\delta\beta}{\delta\kappa_0}(\overline{\kappa}_0) = \frac{\partial\beta}{\partial\alpha}\frac{\partial\alpha}{\partial|\Gamma|}\frac{\delta|\Gamma|}{\delta\kappa_0}. \tag{5.81}$$

However, eigenfunction perturbations of a circular curve $\kappa_0 = \overline{\kappa}$ satisfy $\frac{\delta|\Gamma|}{\delta\kappa_0} = 0$ and the associated eigenvalue problem for $v = \mathrm{e}^{\mu t}\psi(s)$, reduces to

$$\mu\psi = -\left(\partial_s^2 + \overline{\kappa}_0^2\right)^2 \psi. \tag{5.82}$$

As in the analysis of the front-type solution, (3.40), the eigenfunctions are of the form $\psi_n(s) = \mathrm{e}^{\mathrm{i}\xi_n s}$, where $\xi_n = n\overline{\kappa}_0$, for $n = \pm 2, \pm 3, \ldots$, and the associated eigenvalues are

$$\mu_n = -\overline{\kappa}_0^4\left(-n^2+1\right)^2. \tag{5.83}$$

The eigenvalues are all negative for $n \geq 2$, and the radially symmetric curve solution is linearly stable to non-radial perturbations.

5.4.2. Meander Patterns

The evolution Eq. (5.80) also possesses interesting non-radial stationary solutions. Solving $\mathbf{V}_n = 0$ for κ_0 yields the leading-order expression,

$$\partial_s^2 \kappa_0(s) = \beta\kappa_0 - \frac{1}{2}\kappa_0^3. \tag{5.84}$$

This second order equation is Hamiltonian, with conserved quantity

$$E(\partial_s\kappa_0, \kappa_0) = \frac{1}{2}|\partial_s\kappa_0|^2 - \frac{\beta}{2}\kappa_0^2 + \frac{1}{8}\kappa_0^4. \tag{5.85}$$

For $\beta > 0$ there are two bounded solutions corresponding to $E = 0$, a homoclinic orbit which arises out of $(0,0)$, and its negative, which together form a figure eight in the phase plane. For $E > 0$ the stationary solutions, $\kappa_0(s;E)$, can be uniquely parameterized by the value of the energy, E. They form hour-glass shaped periodic orbits about the homoclinic orbits. The corresponding curve $\Gamma_E = \{\gamma(s) | s \in [0, |\Gamma|]\}$ is determined by κ_0 which gives the rate of change of Γ's tangent vector with respect to arc length,

$$\frac{\mathrm{d}\gamma}{\mathrm{d}s} = \begin{pmatrix} -\sin(\theta(s)) \\ \cos(\theta(s)) \end{pmatrix}, \tag{5.86}$$

$$\frac{\mathrm{d}\theta}{\mathrm{d}s} = \kappa_0(s;c). \tag{5.87}$$

The initial conditions on γ and θ determine the rigid body displacement and rotation of Γ_E. For a small value of

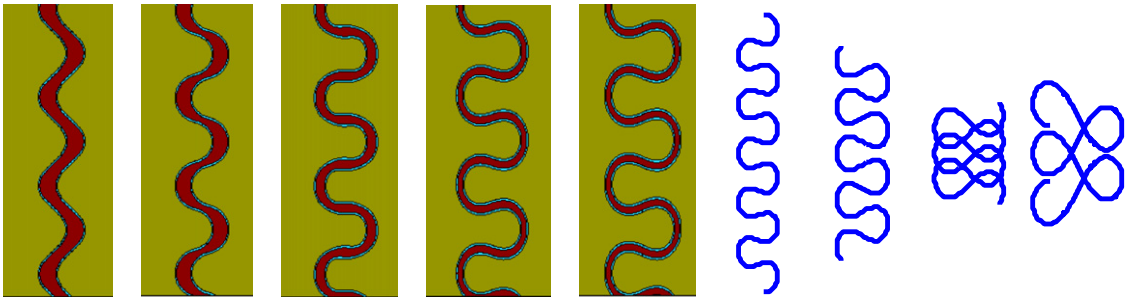

Fig. 5.3. (Left–Right) Development of a meander pattern under the ZMFCH equation with $\eta_2 = 1$ and $\varepsilon = 0.03$. (Far Right) Equal length interfaces Γ integrated from (5.86)–(5.87) using curvatures $\kappa_0(s; H)$ corresponding to periodic solutions of the 2nd order Eq. (5.84) with $\beta = 1$ and three values of $E > 0$. The smallest value of E produces an interface which self-intersects, with increasing values of E decreasing the space-filling nature of the interface's meander.

E the corresponding curve Γ_E is self-intersecting. However for E sufficiently large, depending upon β, the curves do not-self intersect and form *meander* patterns which are stationary equilibria of the evolution system (5.80). Coupling these to the mass constraint (5.38) yields an algebraic system which can be solved for $E > 0$ in terms of the Hamiltonian constant $H > 0$ in terms of the initial data m_0. The meander patterns oscillate about a straight line, and an exact, closed curve solution can be obtained in a periodic square of length L which is tuned to match the spatial periodicity of the particular meander pattern arising from the algebraic system.

Acknowledgements

The third author acknowledges essential support from NSF DMS 0707792, DMS 0929189, and DMS 0934568. He also acknowledges helpful conversations wit Chun Liu when the models were in their early stages of development. This article was completed while the third author enjoyed the hospitality of the mathematics department of the University of Leiden.

Appendix

The linearization L_f of the second order Eq. (3.1) about the single-layer solution ϕ_f enjoys the following properties.

Lemma A.1. *The spectrum of L_f near the origin consists of a single eigenvalue at zero corresponding to the tranlsational eigenfunction ϕ_f'. The remainder of the spectrum of L_f is real and uniformly negative. Moreover the following identities hold,*

$$L_f \phi_f' = 0, \tag{A.1}$$

$$L_f \phi_f'' = W'''(\phi)\left(\phi_f'\right)^2, \tag{A.2}$$

$$L_f(z\phi_f') = 2\phi_f''. \tag{A.3}$$

The linearization L of the second order Eq. (4.15) about its homoclinic solution ϕ enjoys the following properties.

Lemma A.2. *Let $\phi(z;\alpha)$ solve (4.15) with G given by (4.12), then the following equalities hold*

$$L\phi'' = G'''(\phi)\left(\phi'\right)^2, \tag{A.4}$$

$$L\psi_0' = G'''(\phi)\phi'\psi_0 + \lambda_0\psi_0', \tag{A.5}$$

$$L(z\phi') = 2\phi''. \tag{A.6}$$

$$L(z\psi_0) = 2\psi_0' + \lambda_0\psi_0 \tag{A.7}$$

where L linearization of (4.15) about ϕ given in (4.19).

Proof. The first equality follows from taking partial derivatives of (4.15) with respect to z while the second equality arises from taking partial derivative of the eigenvalue equation for ψ_0 with respect to z. The last two equalities follow from expanding the action of L. □

Lemma A.3. *Consider the whiskered mass, $M_b \geq 0$, of the pulse above its background state defined by (5.16). There exists a constant $M_{b,0} > 0$, independent of α, and b for which*

$$M_b(\alpha) = M_{b,0} - \frac{(b_+ - b_-)\|\phi'\|_2^2}{2\gamma_0}\ln(\alpha - \alpha_*) + O(\sqrt{\varepsilon}), \tag{A.8}$$

for $0 < \alpha - \alpha_* \ll \varepsilon^{-\frac{1}{2}}$. In particular M_b is strictly decreasing, everywhere positive, and has a logarithmic singularity as $\alpha \to \alpha_*^+$.

Proof. Taking the α derivative of M_b we see from (4.40) and (4.43) that M_b is strictly decreasing in α,

$$\frac{\mathrm{d}M_b}{\mathrm{d}\alpha} = \int_{\mathbb{R}} \partial_\alpha\phi + \varepsilon^2(\partial_b\phi - 1)\partial_\alpha\hat{b}_2\,\mathrm{d}z = -\overline{\psi_0}\rho_\alpha + O(\varepsilon) < 0. \tag{A.9}$$

Moreover, from (4.26) we have

$$\overline{\psi_0} = -\frac{2\sqrt{2}}{\|\phi'\|_2}\int_0^\infty \phi'\,\mathrm{d}z + O(\sqrt{\varepsilon}) = \frac{2\sqrt{2}(b_+ - b_-)}{\|\phi'\|_2} + O(\sqrt{\varepsilon}), \tag{A.10}$$

so that

$$\frac{\mathrm{d}M_b}{\mathrm{d}\alpha} = -\frac{(b_+ - b_-)\|\phi'\|_2^2}{2(\alpha - \alpha_*)\gamma_0} + O(\sqrt{\varepsilon}), \tag{A.11}$$

from which we deduce (A.8). The positivity of M_b follows from the fact that $\phi > b$ everywhere. □

Lemma A.4. *Consider the inner product $\rho_z(\alpha) \geq 0$ defined by (5.22). There exists a constant $\rho_{z,0} > 0$, independent of α and b such that*

$$\rho_z(\alpha) = \rho_{z,0} - \rho_{\alpha,0}\ln(\alpha - \alpha_*) + O(\varepsilon), \tag{A.12}$$

for $0 < \alpha - \alpha_* \ll \varepsilon^{-1}$.

Proof. First observe that

$$z\psi_0 = -\frac{|z|\phi'}{\|\phi'\|_2} + O(\varepsilon). \tag{A.13}$$

Taking the α derivative and using (4.40) yields

$$z\partial_\alpha\psi_0 = \frac{\rho_\alpha}{\|\phi'\|_2}|z|\psi_0' + O(\varepsilon). \tag{A.14}$$

Taking the α derivative of $\rho_z(\alpha)$ and using the two results above yields

$$\begin{aligned}\partial_\alpha \rho_z(\alpha) &= -(z\partial_\alpha\phi', \psi_0)_2 - (\phi', z\partial_\alpha\psi_0)_2 \\ &= \rho_\alpha \left((z\psi_0', \psi_0)_2 - \frac{1}{\|\phi'\|_2}(\phi', |z|\psi_0')_2 \right) + O(\varepsilon). \quad \text{(A.15)}\end{aligned}$$

However $|z|\phi' = -z|\phi'| = -z\|\phi'\|_2\psi_0 + O(\varepsilon)$ and we obtain

$$\partial_\alpha \rho_z(\alpha) = 2\rho_\alpha(z\psi_0', \psi_0)_2 + O(\varepsilon) = -\frac{\rho_{\alpha,0}}{\alpha - \alpha_*} + O(\varepsilon). \quad \text{(A.16)}$$

Integrating (A.16) in α yields (A.12). □

References

[1] L. Rubatat, G. Gebel, O. Diat, Fibriallar structure of Nafion: matching Fourier and real space studies of corresponding films and solutions, Macromolecules, 2004, 7772–7783.
[2] K. Promislow, B. Wetton, PEM fuel cells: a mathematical overview, SIAM J. Math. Anal. 70 (2009) 369–409.
[3] Kun-Mu Lee, Chih-Yu Hsu, Wei-Hao Chiu, Meng-Chin Tsui, Yung-Liang Tung, Song-Yeu Tsai, Kuo-Chuan Ho, Dye-sensitized solar cells with mirco-porous TiO_2 electrode and gel polymer electrolytes prepared by *in situ* cross-link reaction, Sol. Energy Mater. Sol. Cells 93 (2009) 2003–2007.
[4] J. Peet, A. Heeger, G. Bazan, "Plastic" solar cells: self-assembly of bulk heterojunction nanomaterials by spontaneous phase separation, Acc. Chem. Res. 42 (2009) 1700–1708.
[5] E. Crossland, M. Kamperman, M. Nedelcu, C. Ducati, U. Wiesner, D. Smilgies, G. Toombes, M. Hillmyer, S. Ludwigs, U. Steiner, H. Snaith, A bicontinuous double gyroid hybrid solar cell, Nano Lett. 9 (2009) 2807–2812.
[6] P. Canham, Minimum energy of bending as a possible explanation of biconcave shape of human red blood cell, J. Theoret. Biol. 26 (1970) 61–81.
[7] W. Helfrich, Elastic properties of lipid bilayers—theory and possible experiments, Z. Nat.forsch. C 28 (1973) 693–703.
[8] M. Gurtin, M. Jabbour, Interface evolution in three dimensions with curvature-dependent energy and surface diffusion: interface-controlled evolution, phase transitions, epitaxial growth of elastic films, Arch. Ration. Mech. Anal. 163 (2002) 171–208.
[9] Randall Kamien, The geometry of soft materials: a primer, Rev. Modern Phys. 74 (2002) 953–971.
[10] Chun Liu, Noel Walkington, An Eulerian description of fluids containing visco-elastic particles, Arch. Ration. Mech. Anal. 159 (2001) 229–252.
[11] Qiang Du, Chun Liu, Xiaoqiang Wang, Simulating the deformation of vesicle membranes under elastic bending energy in three dimensions, J. Comput. Phys. 212 (2006) 757–777.
[12] J.W. Cahn, J.E. Hilliard, Free energy of a nonuniform system. I. Interfacial energy, J. Chem. Phys. 28 (1958) 258–267.
[13] R.L. Pego, Front migration in the nonlinear Cahn–Hilliard equation, Proc. R. Soc. Lond. Ser. A 422 (1989) 261–278.
[14] N. Alikakos, P. Bates, X. Chen, Convergence of the Cahn–Hilliard equation to the Hele–Shaw model, Arch. Ration. Mech. Anal. 128 (1994) 165–205.
[15] P. de Mottoni, M. Schatzman, Geometrical evolution of developed interfaces, Trans. Amer. Math. Soc. 347 (1995) 1533–1589.
[16] L. Modica, The gradient theory of phase transitions and the minimal interface criterion, Arch. Ration. Mech. Anal. 98 (1987) 123–142.
[17] P. Sternberg, The effect of a singular perturbation on nonconvex variational problems, Arch. Ration. Mech. Anal. 101 (1988) 209–260.
[18] William Hsu, Timothy Gierke, Ion transport and clustering in Nafion perfluorinated membranes, J. Membr. Sci. 13 (1983) 307–326.
[19] G.M. Grason, C.D. Santangelo, Undulated cylinders of charged diblock copolymers, Eur. Phys. J. E 20 (2006) 335–346.
[20] Dongsheng Wu, Stephen Paddison, James Elliott, Effect of molecular weight on hydrated morphologies of the short-side-chain perfluorosulfonic acid membrane, Macromolecules 42 (2009) 3358–3367.
[21] Klaus-Dieter Kreuer, Stephen J. Paddison, Eckhard Spohr, Micheal Schuster, Transport in proton conductors for fuel-cell applications: simulations, elementary reactions, and phenomenology, Chem. Rev. 104 (2004) 4637–4678.
[22] K. Schmidt-Rohr, Q. Chen, Parallel cylindrical water nanochannels in Nafion fuel cell membranes, Nat. Mater. 7 (2008) 75–83.
[23] S. Paddison, K. Promislow (Eds.), Device and Materials Modeling of Polymer Electrolyte Membrane Fuel Cells, Springer, New York, 2009.
[24] Sangwoo Lee, Manickam A. Arunagirinathan, Frank S. Bates, Path-dependent morphologies in oil/water/diblock copolymer mixtures, Langmuir 26 (2010) 1707–1715.
[25] K. Promislow, H. Zhang, Critical points of functionalized Lagranagians (submitted for publication).
[26] G. Gompper, M. Schick, Correlation between structural and interfacial properties of amphillic systems, Phys. Rev. Lett. 65 (1990) 1116–1119.
[27] Matthias Röger, Reiner Schätzle, On a modified conjecture of De Giorgi, Math. Z. 254 (2006) 675–714.
[28] J. Rubinstein, P. Sternberg, Nonlocal reaction–diffusion equations and nucleation, IMA J. Appl. Math. 48 (1992) 249–264.
[29] P.G. Kevrekidis, C.K.R.T. Jones, T. Kapitula, Exponentially small splitting of heteroclinic orbits: from the rapidly forced pendulum to discrete solitons, Phys. Lett. A 269 (2000) 1357–1377.
[30] Bjorn Sandstede, Arnd Scheel, Gluing unstable fronts and backs together can produce stable pulses, Nonlinearity 13 (2000) 233–277.
[31] Sumeet Jain, Frank Bates, Consequences of nonergodicity in aqueous binary PEO-PB micellar dispersions, Macromolecules 37 (2004) 1511–1523.
[32] Sumeet Jain, Frank Bates, On the origins of morphological complexity in block copolymer surfactants, Science 300 (2003) 460–464.
[33] Xinfu Chen, Spectrum for the Allen–Cahn, Cahn–Hilliard, and phase-field equations for generic interfaces, Comm. Partial Differential Equations 19 (1994) 1371–1395.
[34] Todd Kapitula, Keith Promislow, Stability indices for constrained self-adjoint operators, Proc. Amer. Math. Soc. (in press).
[35] G. Hayrapetyan, K. Promislow, Spectra of functionalized operators, preprint.
[36] K. Promislow, A renormalization method for modulational stability of quasi-steady patterns in dispersive systems, SIAM J. Math. Anal. 33 (6) (2002) 1455–1482.
[37] R. Moore, K. Promislow, Renormalization group reduction of pulse dynamics in thermally loaded optical parametric oscillators, Physica D 206 (2005) 62–81.